
Audits Under Resource, Data, and Access Constraints: Scaling Laws For Less Discriminatory Alternatives

Sarah H. Cen
 Stanford University
 Palo Alto, CA 94304
 shcen@stanford.edu

Salil Goyal
 Stanford University
 Palo Alto, CA 94304
 salilg@stanford.edu

Zaynah Javed
 Stanford University
 Palo Alto, CA 94304
 zjaved@stanford.edu

Ananya Karthik
 Stanford University
 Palo Alto, CA 94304
 ananya23@stanford.edu

Percy Liang
 Stanford University
 Palo Alto, CA 94304
 pliang@cs.stanford.edu

Daniel E. Ho
 Stanford University
 Palo Alto, CA 94304
 deho@stanford.edu

Abstract

AI audits play a critical role in AI accountability and safety. One branch of the law for which AI audits are particularly salient is anti-discrimination law. Several areas of anti-discrimination law (including but extending beyond employment) implicate what is known as the “less discriminatory alternative” (LDA) requirement, in which a protocol (e.g., model) is defensible if no less discriminatory protocol that achieves comparable performance can be found with a reasonable amount of effort. Notably, the burden of proving an LDA exists typically falls on the claimant (the party alleging discrimination). This creates a significant hurdle in AI cases, as the claimant would seemingly need to *train* a less discriminatory yet high-performing model, a task requiring resources and expertise beyond most litigants. Moreover, developers often shield information about and access to their model and training data as trade secrets, making it difficult to reproduce a similar model from scratch.

In this work, we present a procedure enabling claimants to determine if an LDA exists, even when they have limited compute, data, information, and model access. To illustrate our approach, we focus on the setting in which fairness is given by demographic parity and performance by binary cross-entropy loss. As our main result, we provide a novel *closed-form* upper bound for the loss-fairness Pareto frontier (PF). This expression is powerful because the claimant can use it to fit the PF in the “low-resource regime,” then extrapolate the PF that applies to the (large) model being contested, all without training a single large model. The expression thus serves as a *scaling law* for loss-fairness PFs. To use this scaling law, the claimant would require a small subsample of the train/test data. Then, for a given compute budget, the claimant can fit the context-specific PF by training as few as 7 (small) models. We stress test our main result in simulations, finding that our scaling law applies even when the exact conditions of our theory do not hold.

1 Introduction

Complex AI systems are increasingly used in decision-making contexts that are subject to legal oversight. For example, HireVue has used AI to score video interviews [30]; various US agencies apply facial recognition for fraud detection [3, 4, 5]; and insurance providers use elaborate behavioral data to price policies [45, 46]. In the absence of methods that test whether such systems comply with the law, decisions that rely heavily on AI are permitted to escape scrutiny, unless one can establish

wrongdoing through other means such as showing intent to harm. Accordingly, there is growing need for AI audits. This need is particularly pronounced as models increase in complexity and scale. For instance, one challenge in AI audits is selecting the samples on which to evaluate an AI system. The number of possible samples to test increases exponentially with the input dimension, which presents a challenge as decision makers shift from applying AI on low-dimensional feature vectors to doing so on high-dimensional, unstructured text and video. We henceforth refer to the system being audited as the “model,” noting our analysis applies broadly, e.g., to human-AI decisions.¹

AI audits are particularly salient in anti-discrimination law, in which the goal is typically to determine whether a protocol discriminates on the basis of a protected attribute. In the US, numerous laws concern discrimination, including the Equal Credit Opportunity Act, Fair Housing Act, Americans with Disabilities Act, and Title VII of the Civil Rights Act. Although these laws do not explicitly mention AI, models used in these decision-making contexts are subject to scrutiny. There are additionally efforts to regulate automated systems directly, such as NYC’s Local Law 144, which requires annual bias audits of “automated employment decision tools,” including AI.

Several areas of anti-discrimination law implicate the “**less discriminatory alternatives**” (**LDA requirement**). Conceptually, it holds that a protocol (e.g., AI model) should not be used if a protocol that achieves comparable performance while being less discriminatory can be found without causing “undue hardship” (i.e., imposing significant costs on the employer). The LDA requirement arose from an understanding that there may be trade-offs between equity and considerations such as performance and cost (cf. Sections 2 and 7). When such trade-offs exist, the courts may wish to understand why a discriminatory outcome occurs and thus consider equity alongside other factors. In this way, this requirement is more flexible than thresholds (e.g., requiring that a measure of discrimination not exceed a certain value). For most of this work, we ground our discussion in a well-known context involving LDAs: Title VII of the US Civil Rights Act. Importantly, under Title VII, the burden of proving that an LDA exists *falls on the plaintiff*.

The LDA requirement highlights a fundamental and recurring issue in AI audits that is at the heart of our work: claimants generally have *fewer resources, less expertise, and limited knowledge* about the audited model than the defendants they challenge, and yet *bear the burden of proof*. We refer to this phenomenon as the “**resource-information asymmetry**” in AI evidence production.

This asymmetry can prevent claimants from gathering enough evidence to substantiate their claims under current legal standards. The LDA requirement drives this point home. Interpreted straightforwardly, the claimant is asked to *provide* a less discriminatory model, i.e., train a model that maintains the same level of performance as state-of-the-art, production models while simultaneously reducing discrimination. However, most claimants lack the compute, data, and expertise to do so. To add to the asymmetry, developers fiercely protect their models, training procedures, and data as trade secrets, meaning that claimants wishing to train a comparable model lack critical information. Thus, in the absence of methods enabling claimants to establish the existence of LDAs under this asymmetry, the LDA requirement may block their primary (sometimes, only) path to accountability.²

1.1 Contributions

In this work, we tackle the resource-information asymmetry, using the LDA requirement as our case study. As is customary in disparate impact analyses, we focus on the classification setting (noting that this *includes* decisions that use generative AI to classify individuals). While our primary objective is to provide tools that equip claimants with the ability to substantiate their claims, we note that our approach *also helps model developers* assess the existence of LDAs without expending significant resources (since our method is specifically designed to require minimal resources).

¹We adopt this terminology to simplify our language. Using “model” to refer to the broader AI system that results from pre-training, post-training, guardrailing, etc. is increasingly common. For our purposes, the most relevant question is whether our analysis applies to AI-assisted decisions in which humans are also involved, as this setting arises frequently, to which the answer is *yes*. One would simply use the appropriate outcome/decision in all salient calculations, e.g., when computing loss and fairness.

²Under Title VII, the disparate impact doctrine is often favored for claims brought against automated or AI-assisted decisions. However, a successful disparate impact claim requires establishing the existence of an LDA (as the final step), meaning that the resource-information asymmetry in evidence production can block what may be the only viable path a claimant has to prevail in a Title VII disparate impact case.

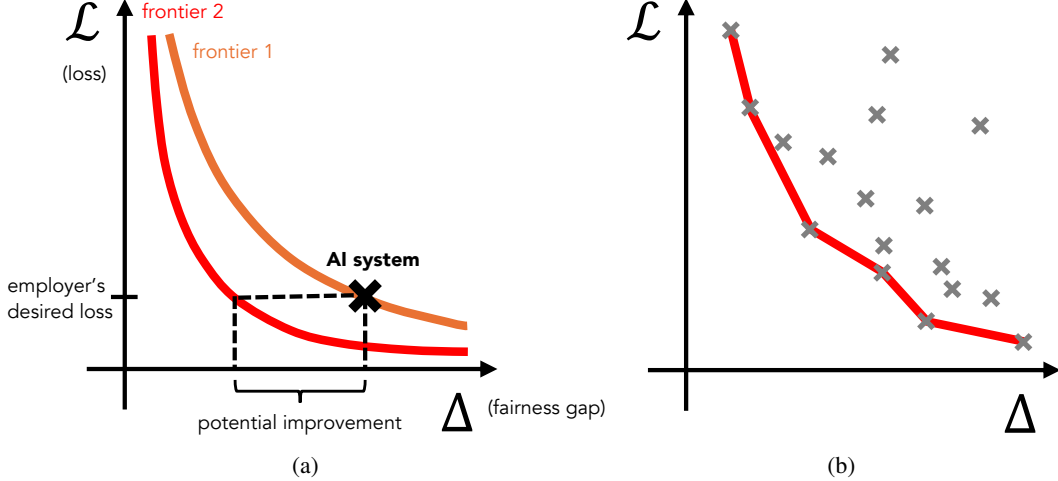


Figure 1: (a) Consider the contested AI model, as given by the “X” on the loss vs. fairness gap plane. As described in Section 2, there are two steps in a disparate impact case before the less discriminatory alternatives (LDA) step. In the first step, the claimant establishes that there is disparate impact, typically by pointing to a statistical measure of discrimination (the fairness gap). Thus, the first step identifies the x-coordinate of the model (of “X”). In the second step, the defendant counters by arguing that the disparity serves what is known as business necessity, demonstrating that it allows them to meet some desired performance (the y-coordinate of “X”). In the third and final step, the claimant must prove that the employer could have used an LDA that would be less discriminatory while still meeting the employer’s desired performance (i.e., a model that is to the left of but no higher than “X”). In this work, we cast this problem as determining where the performance-fairness Pareto frontier (PF) lies. For example, if the PF is given by the orange curve, then the “X” is on the PF, meaning that no LDAs exist; to decrease the fairness gap, one must sacrifice performance. If the PF is given by the red curve, there is significant room to improve fairness while maintaining performance. Note that, this figure abstracts away several nuances, which are further discussed in our work. (b) However, recasting the problem to finding the PF does not immediately resolve the resource-information asymmetry. The typical approach is to train many models while inducing them to have different loss-fairness characteristics, as given by the small x’s, then trace the curve connecting the points lowest and to the left, as given by the red line. The issue is: for the PF to apply, the trained models must be of comparable size to the contested model. Training such models requires resources, data, and expertise beyond most claimants. Our work provides a cost-effective way to find the PF.

Conceptually, we first shift the problem from that of *training* a less discriminatory model to showing that a less discriminatory model *exists*, as explained in Section 2 and visualized in Figure 1a. We thus recast the problem to one of finding the performance-fairness Pareto frontier (PF). If the contested model sits far from the PF, then many LDAs exist. One could therefore measure how easily the defendant would be able to obtain an LDA using the distance from the PF, as we formalize in Section 3. An additional benefit of this approach is that finding the PF does not reveal information specific to the contested model. Note that, to use PFs, one must be able to quantify performance and fairness in some way; although not always possible, this is rarely prohibitive because disparate impact analyses of AI generally involve quantitative evidence, even if no single metric is determinative.³

Recasting the problem in terms of PFs does not immediately resolve the resource-information asymmetry because finding the PF is a challenging problem in and of itself (see Figure 1b). Existing methods for finding the PF are just as (often *more*) resource-intensive than producing an LDA (see Sections 2 and 7). Our approach transforms this task into a tractable one by finding a scaling law for the performance-fairness PF, as visualized in Figure 2. Given the form of the scaling law, claimants could first fit parameters of the scaling law in a low-resource environment, then extrapolate where the PF falls for the contested (large) model. Thus, the claimant would never need to train a large

³Under disparate impact doctrine, the goal is to show that different groups experience disparate outcomes, and defendants can counter by arguing that this disparity is necessary for business reasons. To do so, both sides generally present quantitative evidence (cf. the Four-Fifths rule), especially when the claim concerns an algorithmic/automated system. In fact, much of the field of algorithmic fairness relies on the ability to present quantitative evidence, where the appropriate metric is context-dependent. Moreover, to establish that a protocol (such as a model) is less discriminatory, one must typically specify what constitutes “less” or “more,” making quantitative evidence more compelling.

model. Such a scaling law would allow several types of analyses, such as (i) estimating how far the contested model is from the PF for models of equivalent size trained on a similar amount of data; or (ii) alternatively, estimating how many resources one would need to obtain a model with specific performance-fairness attributes. In addition to requiring fewer resources, this approach requires minimal information about the contested model, bypassing barriers created by trade secrecy.

This approach hinges on the existence of a scaling law. We provide, to our knowledge, the first *closed-form upper bound* of a performance-fairness PF (that is also, in a sense, tight). We describe how this expression can be used as a scaling law that allows one to learn the PF empirically at a fraction of the cost of existing methods. Our result uses binary cross-entropy loss as our performance metric, demographic parity as our fairness metric, and a posited data-generating process, as given in Sections 3 and 4. We hope to extend this result to other fairness and performance metrics in future work. As mentioned above and described in Section 5, to apply the scaling law, one needs four ingredients: (i) test data for evaluation, (ii) a small subsample of the training data, (iii) an estimate of the contested model’s size, and (iv) an estimate of the amount of data used to train the contested model. Of these, (i) should not be difficult to obtain, as both parties use test data for the two steps of disparate impact cases preceding the LDA step (see Section 2). While the defendant must provide (ii)-(iv), they are more conservative asks than the status quo and may thus help strike a balance between the plaintiff’s and defendant’s interests.⁴

We conclude with experiments on synthetic data to stress test the conditions of our theoretical result. Specifically, our result uses assumptions on the data-generating process and an assumption on the PF (that models on the PF satisfy a certain notion of symmetry, where this is *not* a condition on all models, just on Pareto-optimal ones). We find that our scaling law holds even when the conditions of our theory do not. We emphasize that our method is plug-and-play: as researchers develop better methods for finding Pareto-optimal models, our approach provides increasingly better estimates.

Our main contributions are summarized as follows:

1. We cast the problem of establishing the existence of an LDA and/or estimating the cost of producing an LDA as determining the performance-fairness Pareto frontier (PF).
2. We provide a closed-form upper bound of the performance-fairness PF that functions as a scaling law. We describe how one would apply this scaling law to determine whether an LDA exists at a fraction of the cost of both training a large model.
3. We conduct small-scale experiments to test our theoretical result.

Finally, we note that although we study LDAs, we believe that the need for low-resource, low-information methods to substantiate AI claims and conduct AI audits is a broad and pervasive issue. We point out extensions to our work in Section 8 and Appendix A.

2 Less Discriminatory Alternatives and Their Relation To Pareto Frontiers

In this section, we discuss the relation between less discriminatory alternatives (LDAs) and Pareto frontiers (PFs). To scope our analysis, we situate ourselves in the context of Title VII of the US Civil Rights Act (CRA). Our analysis will allow us to map the LDA requirement to a formal problem statement in Section 3, in which a claimant seeks to determine whether an LDA exists with limited resources and limited information about the contested model. A more extensive background and related work can be found in Section 7.

2.1 Three steps of disparate impact cases

In the US, Title VII of the US CRA prohibits employment discrimination on the basis of race, color, religion, sex, and national origin, which are often referred to as “protected attributes.” Although there are several ways to litigate under Title VII, the legal theory that is typically applied to automated

⁴Straightforward approaches to finding an LDA require access to the trained model (e.g., to use it as a starting point from which one searches locally for an alternative) and/or a significant portion of its training data (e.g., to train a comparable model). Alternate methods that do not require access or data generally assume low-dimensional, categorical inputs that are not reflective of contemporary applications of complex, generative AI to unstructured, high-dimensional inputs.

decisions is the disparate impact doctrine [8, 33].⁵ Courts generally adopt a three-part, burden-shifting test to adjudicate disparate impact claims:

1. The plaintiff must show that a facially neutral employment practice has *disparate impact* on a protected class, i.e., leads to systematically different outcomes for individuals on the basis of a protected attribute. For automated systems, this is generally done by showing a statistical disparity in outcomes between different groups, which means that a quantitative notion of discrimination is adopted at this step of the case.
2. If the plaintiff successfully establishes disparate impact, the defendant (e.g., employer or employment agency) can counter by showing that the practice is for “*business necessity*” reasons: that it is demonstrably related to an important and legitimate business goal. Similarly to the above, a quantitative notion of the business goal is often adopted.
3. If the defendant successfully claims business necessity, the burden of proof shifts back to the plaintiff for the third and final step. The plaintiff must prove that there is a *less discriminatory alternative (LDA)*: a protocol that the defendant could find without undue hardship and that would serve the same employment goal as in Step 2 while causing less disparate impact. Unless the plaintiff is able to meet this LDA requirement, the plaintiff loses the case.

Our work addresses **Step 3**. We assume Step 1 (which is studied extensively by the algorithmic fairness community [21, 63, 27, 18, 23]) and Step 2 are complete. See Section 7 for further discussion.

2.2 Example: Challenges of finding an LDA

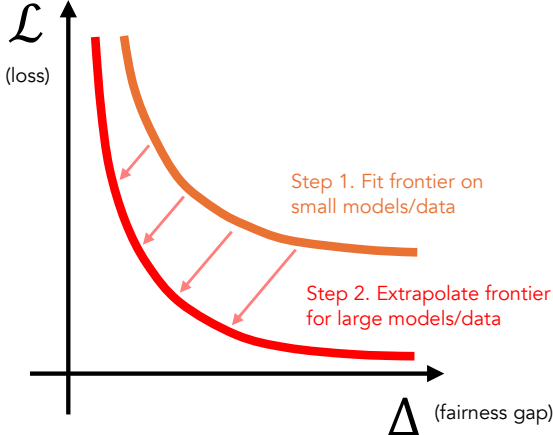
To illustrate the challenges involved in finding an LDA, consider the following example. Consider an AI tool that uses large language and video models to screen application packages, which contain unstructured text and video interviews. Suppose that the plaintiff successfully establishes that the tool disproportionately favors candidates from a specific demographic group using one or more chosen metrics, such as the demographic parity gap (Step 1). Suppose further that the defendant successfully shows that the tool improves their business outcomes by reducing the amount of time to screen applicants while surfacing candidates that are well suited for each job (Step 2).

At this point, the plaintiff can only win the case if they are able to meet the LDA requirement (Step 3). They meet several hurdles in their attempts:

1. The plaintiff first attempts to train their own LDA. They quickly realize that training a comparable model to the defendant’s production, state-of-the-art model requires significant compute.
2. Even if they are able to obtain the necessary compute, training a model requires access to good data. The plaintiff learns that collecting enough training data is prohibitively expensive, so the plaintiff requests it from the defendant (or the developer if the data is owned by a third party). The defendant and/or developer claims that sharing their training data is tantamount to releasing trade secrets and compromises user privacy, and the judge agrees.⁶
3. The plaintiff turns to a third option. They request access to the contested model so that they can use it as a starting point to locally search for an LDA by, e.g., fine-tuning or probing its internal representations. The defendant and/or developer claims that this, too, violates trade secrecy, and the judge agrees.

⁵The other well-known legal theory is disparate treatment, which applies when a decision-maker intentionally treats an individual differently based on their protected class. In contrast, disparate impact applies when a facially neutral practice has a disproportionate effect on individuals belonging to a protected class. Disparate treatment thus relies on the existence of intent while disparate impact shifts the focus to the outcome or effects of an employment practice. In the context of automated decision-making and AI systems, disparate impact is typically applied due to the difficulty of ascribing intent to algorithms or models [8]. Although disparate treatment is not generally applied to automated and AI systems, some have begun to contemplate its application due to the rise of “reasoning” models that seem to verbalize “intent.” In addition, some believe that algorithms that use protected attributes as inputs should be subject to a disparate treatment analysis.

⁶Requesting access to information about models, data, and training procedures is a complex issue. This information is often protected as proprietary. When the owner of the information is a third party that is not a direct party to the lawsuit (e.g., the plaintiff sues an employer, who outsources the AI model development to a third party), it can be even more difficult to obtain this information. Further discussion in Footnote 12.



Scaling law for loss-fairness PFs

How does this approach address the resource-information asymmetry?

Information asymmetry. Claimants are often denied access to the model, data, and information about the training procedure. The PF is not model-specific and thus does not require knowledge about the contested model that may be considered proprietary.

Resource asymmetry. Current methods for finding a PF are costly (require training many large models → more resource-intensive than finding an LDA). Using a scaling law means the claimant never needs to train a large model.

Figure 2: An illustration of the proposed method on the left and how it addresses the resource-information asymmetry on the right, as explained in Section 2.

- Finally, the plaintiff considers establishing the existence of an LDA by characterizing the range of possible classifiers, in the same spirit as analyses in [24, 40], but discovers these approaches work well on finite-dimensional, categorical inputs but not on unstructured ones.

At this point, the plaintiff may throw in the towel, conceding that they cannot meet the LDA requirement because the burden of providing an LDA is too high, especially given the limited resources, data, and model access that they possess.⁷

2.3 Relation between LDAs and Pareto frontiers

The example above highlights the difficulties of providing an LDA given the resource-information asymmetry. However, the LDA requirement does not necessarily imply that the plaintiff must train a new model. Instead, the plaintiff can prove, to a sufficient standard, that such an alternative exists.⁸

In Figure 1a, we illustrate how proving the availability and feasibility of an LDA can be cast as determining that a given model lies far from the performance-fairness PF. Specifically, when the defendant's model does not lie on the PF, then there exists a model that is less discriminatory but equally effective, where the distance from the PF is related to the "hardship" of finding the LDA, as formalized in the following section. Intuitively, under the mild assumption that the Pareto frontier "improves" as the cost/effort budget increases, then distance from the PF characterizes the amount of cost/effort needed to find an LDA with certain performance-fairness characteristics. Recasting the LDA requirement as a problem of finding the PF helps to address the **information asymmetry** problem: proving an LDA's availability and feasibility does not hinge on specific knowledge that is considered the defendant's or developer's proprietary information.⁹

However, this recasting does not immediately resolve the **resource asymmetry**. In fact, the general method for finding the PF is to train a wide array of models with varying performance-fairness characteristics, plot them on the performance-fairness plane, and then trace out the empirical PF [21, 61, 6], as illustrated in Figure 1b. From a resource perspective, this is *more* difficult than training

⁷Note that there are other options that would not require the plaintiff to train their own model, such as showing that a competing product is less discriminatory but equally effective. Although such a situation would be helpful, we do not assume that there exists a competitor that meets these criteria.

⁸We cannot say for certain how courts will receive this evidence. If courts believe it meets the evidentiary standard, then the plaintiffs can satisfy the LDA requirement without actually training an LDA. Even if courts do not believe it fully satisfies the LDA requirement, it can be used to as an intermediate step that supports the plaintiff's requests for further discovery, including data and model access that they may be initially denied (see points 2 and 3 in Section 2.1).

⁹It is important to note that, while similar to what is described in point 4 of Section 2.1, our approach is distinct in that it works on high-dimensional, unstructured inputs.

a single large model—it involves training many! Our main technical contribution, as outlined in Figure 2, is a scaling law that greatly reduces the resource cost of finding the PF.

3 Formal Problem Statement

In the remainder of this work, we demonstrate a method for proving the existence of a less discriminatory alternative (LDA) in a low-resource, low-information setting.

3.1 Setup

Consider a binary classification setting, where random variables $X \in \mathcal{X}$, $A \in \{0, 1\}$, and $Y \in \{0, 1\}$ denote the features, (binary) sensitive attribute, and (binary) class of an individual. Notably, X may be unstructured. For instance, X could denote a job applicant’s resume, A their sex, and Y their suitability for the job of interest. Throughout, we use the convention that capital letters represent random variables, and their lower-case analogs denote specific values that they can take. Let $f : \mathcal{X} \times \{0, 1\} \rightarrow [0, 1]$ denote a (soft) classifier that takes in features x and sensitive attribute a and returns a score $f(x, a)$ between 0 and 1. Note that having f depend on a is without loss of generality, as f could ignore it, so we use this A -“aware” setup. We use \mathcal{F} to denote the model class (e.g., neural network of size N) that f belongs to and \mathcal{D} to denote f ’s training dataset.

In this work, we use (expected) binary cross-entropy (BCE) loss as our measure of performance. Let the BCE of f with respect to a (fixed) joint distribution $p_{X, A, Y}$ be given by

$$\mathcal{L}(p_{X, A, Y}, f) := -\mathbb{E}_{x, a, y \sim p_{X, A, Y}} [y \log(f(x, a)) + (1 - y) \log(1 - f(x, a))]. \quad (1)$$

We use demographic parity as our notion of fairness. Thus, the fairness gap of f with respect to a conditional distribution $p_{X|A}$ is given by

$$\Delta(p_{X|A}, f) := |\mathbb{E}_{x \sim p_{X|A=1}} [f(x, 1)] - \mathbb{E}_{x \sim p_{X|A=0}} [f(x, 0)]|.$$

We refer to p as the “test” distribution. Note that the plaintiff may choose to use other notions of performance and fairness. In this work, we use BCE and demographic parity, leaving an analysis of other definitions to future work.¹⁰ The “right” choice of fairness metric is generally context-dependent and highly debated. History indicates that demographic parity is a likely choice by courts, as selection rates (the backbone of the demographic parity metric) have appeared across multiple contexts, including the Four-Fifths Rule from 1978 to NYC’s Local Law 144 of 2021. Moreover, selection rates do not suffer from the same selection bias issues as other metrics (see Section 7 for further discussion). Similarly, we study BCE loss because it is widely used as the performance metric for classifiers and is precisely what developers/companies optimize in training.

3.2 Our objective: Establishing existence of an LDA with limited information and resources

Limited resources. Suppose the plaintiff’s model belongs to a model class \mathcal{F}^- and is trained on a dataset \mathcal{D}^- , which are much smaller than the model class \mathcal{F}^+ and training dataset \mathcal{D}^+ available to the defendant. Let N^+ and D^+ denote the parameter count of \mathcal{F}^+ and number of samples in \mathcal{D}^+ . Similarly, let N^- and D^- denote the parameter count of \mathcal{F}^- and number of samples in \mathcal{D}^- . Suppose that the claimant can only train models that belong to \mathcal{F}^- and \mathcal{D}^- , where $N^+ \gg N^-$ and $D^+ \gg D^-$. We assume that \mathcal{D}^- is drawn from the same distribution as \mathcal{D}^+ .

Limited information. In past and ongoing cases, judges and defendants have been reluctant to share information about the model and training data, arguing that this information is proprietary and confidential.¹¹ In this work, we assume the claimant is similarly denied access to the contested model but can request a limited amount of information. We propose that, since the LDA requirement asks that the claimant assess what alternatives are “feasible” or “reasonable” for a defendant to obtain, the

¹⁰Importantly, recall from Section 2 that the plaintiff chooses their definition of disparate impact in Step 1 and the defendant chooses their definition of business necessity/legitimate employment goal in Step 2. By the time the plaintiff arrives at Step 3, they can inherit the definitions chosen in Steps 1 and 2, since presumably the parties of the case and judge have reached agreement on these definitions in order to arrive at Step 3.

¹¹In some cases, the developer is actually a third party that is not a direct party to the lawsuit. This can make it even more difficult to obtain potentially proprietary information about the model, data, and training procedures.

claimant should minimally be given information about how many resources were used to train the contested model: namely, the values N^+ and D^+ . We further propose that the claimant should be granted a small subsample of training and test data. In the notation given above, the subsample of training data would be of size D^- , and the subsample of test data at most D^- .¹²

Objective: Show existence of a (feasible) LDA. Our objective is to provide a method that the claimant can use to determine whether the contested model is at least δ -far from the Pareto frontier (PF) for a fixed performance level (i.e., loss), which would imply that finding an LDA is δ -feasible.

Formally, let the defendant’s contested model be denoted by \hat{f}^* . Our objective is to provide a method that the claimant can use to determine whether, for a given value $\delta > 0$, there exists a model \hat{f} of size N^+ and trained on a dataset of size D^+ such that

$$\mathcal{L}(p_{X,A,Y}, \hat{f}) \leq \mathcal{L}(p_{X,A,Y}, \hat{f}^*) \quad \text{and} \quad \Delta(p_{X|A}, \hat{f}) < \Delta(p_{X|A}, \hat{f}^*) - \delta. \quad (2)$$

In other words, there exists a model that is at least as performant as the contested model and reduces the contested model’s fairness gap by at least $\delta > 0$. The larger the value of δ , the greater the distance between the contested model and the PF.

This distance is indicative of the “feasibility” of finding an LDA: under the mild assumption that the loss-fairness PF monotonically improves as N and D increase (which our result and experiments support), large values of δ indicate that the defendant could have found an LDA with a small fraction of the resources they expended to train \hat{f}^* . Our scaling law will allow us to estimate the minimal N and D needed to achieve certain loss-fairness characteristics.

4 Main Result: Scaling Law for Loss-Fairness Pareto Frontier

In this section, we derive a scaling law for the loss-fairness Pareto frontier (PF) under a given data generating process (DGP). We then describe how one applies this scaling law. All proofs are given in Appendices C and D.

4.1 Intermediate result

We begin with an intermediate result that characterizes BCE loss for any DGP. A reader interested only in our main result (the scaling law) may wish to skip ahead to Section 4.2. We present this intermediate result for two reasons. First, it lends intuition for how our main result is obtained. Second, it does not depend on a specific definition of fairness or the DGP; it can therefore be used as a building block for future works that examine different notions of fairness and DGPs.

Before presenting the result, we introduce some notation. Let p and q denote joint distributions over random variables X , A , and Y . Let $p(1 | x, a)$ and $q(1 | x, a)$ denote the Bayes optimal classifiers under p and q , respectively. Let $\text{KL}(\cdot, \cdot)$ denote the Kullback-Liebler divergence. The result below simply decomposes the loss of a classifier \hat{f} on a test distribution p into three components. For reasons that will become clear in the following section, we state this result in terms of p and an auxiliary distribution q .

Lemma 4.1. *Consider a classifier $\hat{f} : \mathcal{X} \times \mathcal{A} \rightarrow [0, 1]$. Consider arbitrary joint distributions p and q over X , A , and Y , where $p_{X,A,Y} \ll q_{X,A,Y}$. Let $S(x, a, y) := y \log(q(1 | x, a) / \hat{f}(x, a)) + (1 - y) \log((1 - q(1 | x, a)) / (1 - \hat{f}(x, a)))$ be absolutely integrable. We assume $\mathbb{E}_{p_{X,A,Y}}[S(x, a, y)] = \mathbb{E}_{q_{X,A,Y}}[S(x, a, y)]$. Then,*

$$\begin{aligned} \mathcal{L}(p_{X,A,Y}, \hat{f}) &= (\mathcal{L}(q_{XAY}, \hat{f}) - \mathcal{L}(q_{XAY}, q_{1|X,A})) \\ &\quad + \mathbb{E}_{x,a \sim p_{X,A}} [\text{KL}(p_{Y|x,a} \| q_{Y|x,a})] + \mathcal{L}(p_{X,A,Y}, p_{1|X,A}). \end{aligned} \quad (3)$$

Interpretation. This result decomposes the loss of an arbitrary classifier \hat{f} on a test distribution p into three components: (1) the misspecification loss due to the choice of model class \mathcal{F} ; (2) the

¹² This amount of information is more conservative than what has been requested in past cases [2, 49] and what practitioners currently advocate for [16, 17]. As such, although one may argue that any information about the model and data used to train it is proprietary/confidential, we believe that this level of access is modest and, in the absence of any information, claimants are powerless.

loss due to distribution shift between p and q ; and (3) the irreducible test loss given by the BCE loss of the Bayes optimal classifier $p_{1|X,A}$ on $p_{X,A,Y}$, where $p_{1|X,A}$ denotes the classifier that returns $p_{1|X,A}(x, a)$ on (x, a) . This result follows from a simple telescoping sum that utilizes the definitions of information theoretic terms and the stated condition involving S .

Why is this useful? Recall that our goal is to derive a scaling law of the loss-fairness PF. That is, our goal is to produce a closed-form expression of loss, which is the left-hand side of (3), in terms of the fairness gap of \hat{f} on p . Theorem 4.1 gets us part of the way there; the next step is to write the right-hand side of (3) in terms of the chosen fairness gap for a given DGP.

Understanding the condition on \hat{f} . We briefly comment on the condition $\mathbb{E}_{p_{X,A,Y}}[S(x, a, y)] = \mathbb{E}_{q_{X,A,Y}}[S(x, a, y)]$, which is a condition on \hat{f} . We observe that S is the log likelihood ratio between Bernoulli models $q(1|x, a)$ and $\hat{f}(x, a)$, such that $\mathbb{E}_{q_{X,A,Y}}[S(x, a, y)]$ is the expected conditional KL divergence between them. In the next section, Theorem 4.2 implicitly asks that this condition hold across all q 's that we consider, which implies that $\mathbb{E}_{q_{X,A,Y}}[S(x, a, y)]$, i.e., that the “distance” (as given by an expected log likelihood ratio) between \hat{f} and the Bayes optimal $q(1|x, a)$ is constant.

When would we expect this to hold true and is it restrictive? One might expect this to hold true if \hat{f} is the model that results from training on q . If \hat{f} is the result of training on q , then the condition asks that the training procedure and model class result in an \hat{f} that replicates the patterns in its train distribution equally well, regardless of train distribution. In practice, we do not expect this condition to hold exactly; the training procedure and model class may fit some q 's better than others, e.g., if there exists a q that is trivial to learn. However, we believe this is a reasonable condition for large models trained on sufficiently sophisticated tasks because deep learning models are designed to serve as universal function approximators across different distributions.

Importantly, we emphasize that q is *not* the true train distribution. As explained in the following section, q is an artificial, auxiliary distribution that gives rise to our main proof technique.

4.2 Main result: Closed-form upper bound of the loss-fairness Pareto frontier

Recall that a Pareto frontier (PF) is traced out by the lowest-loss classifier for every fairness gap value $\underline{\Delta}$. In this section, we present our main result: a closed-form upper bound of the loss-fairness PF. We begin with an assumption.

Assumption 4.2 (Model misspecification symmetry). For a given distribution q , let \hat{f} be the loss-minimizing classifier in model class \mathcal{F} when training on a dataset \mathcal{D} drawn from q . We assume that $\mathcal{L}(q_{XAY}, \hat{f}) - \mathcal{L}(q_{XAY}, q_{1|X,A})$ is a constant $c_1(\mathcal{F}, D)$, that does not depend on q or \hat{f} . Moreover, $\mathbb{E}[\hat{f}(x, A)|A = 0] - \mathbb{E}[q(1|x, A)|A = 0] = \mathbb{E}[\hat{f}(x, A)|A = 1] - \mathbb{E}[q(1|x, A)|A = 1]$, where all expectations are taken with respect to the test distribution $p_{X|A}$.

This assumption essentially implies that each Pareto-optimal model \hat{f} that belongs to model class \mathcal{F} is symmetric with respect to the DGP, which one would expect to hold for large models that serve as universal function approximators. That is, the “distance” between the loss-minimizing \hat{f} in \mathcal{F} learned on q and the Bayes optimal classifier $q(1|x, a)$ may depend on the model class \mathcal{F} and the number of samples D it is trained on, but not on q . As discussed in the previous section, this may not always hold exactly (e.g., when some q 's are trivial to learn), but we believe it to be reasonable for deep learning models trained on sufficiently sophisticated tasks. The second condition in Theorem 4.2 implies that \hat{f} is symmetric with respect to A . This condition does *not* imply that \hat{f} fits group $A = 0$ as well as the other group $A = 1$, but that the “distance” between \hat{f} and $q(1|x, a)$ is symmetric with respect to A ; to see this, observe that it “compares” \hat{f} to the Bayes optimal classifier for q , which itself may be skewed.¹³

We now present our main result.

Theorem 4.3. *Consider the following data generating process: $A \sim \text{Ber}(\pi)$, $X \perp A$, and $Y|X, A \sim \text{Ber}(\sigma(g(X) - \zeta A))$ for $\zeta \geq 0$, where $\sigma(\cdot)$ is the sigmoid function, g is a measurable function, and q is the joint distribution induced by some ζ . With slight abuse of notation, let $\underline{\Delta} := \Delta(p_{X|A}, \hat{f})$*

¹³The second condition can be loosened to be equality with a constant shift, but we remove this for simplicity. It will introduce additive constants throughout our proof that are ultimately incorporated into the constants and thus do not affect the main result.

denote the fairness gap of \hat{f} under test distribution p . We assume $p = q^{\zeta_p}$ for a fixed ζ_p and all Pareto-optimal \hat{f} satisfy Theorem 4.2 for some q^ζ . Then, for all \hat{f} on the Pareto frontier,

$$\begin{aligned} \mathcal{L}(p_{X,A,Y}, \hat{f}) &\leq B(\mathcal{F}, D) - c \cdot c' \log(1 - c'' + \underline{\Delta}) - c \cdot (1 - c') \log(c'' - \underline{\Delta}) \\ &\quad + (c'' - \underline{\Delta})(1 - c'' + \underline{\Delta}) \left(\frac{c \cdot c'}{2(1 - c'' + \underline{\Delta})^2} + \frac{c \cdot (1 - c')}{2(c'' - \underline{\Delta})^2} \right) + \varepsilon, \end{aligned} \quad (4)$$

where $\varepsilon = \mathcal{O}(\max_\zeta \mathbb{E}_{p_{X|A}=1} [(q_{Y|X,A}^\zeta(1|x,1) - \bar{q}_1^\zeta)^3])$ and $\bar{q}_1^\zeta := \mathbb{E}_{p_{X|A}=1} [q_{Y|X,A}^\zeta(1|x,1)]$. $B(\mathcal{F}, D)$ is a constant that depends on the model class \mathcal{F} , dataset size D and p , and $c, c', c'' \in [0, 1]$ are constants that depend only on p .

Interpretation. This result expresses the loss of each Pareto-optimal \hat{f} on p as a function of \hat{f} 's fairness gap $\Delta(p_{X|A}, \hat{f})$ on p . The dependence of loss on fairness gap is fully characterized, except for four constants $B(\mathcal{F}, D)$, c , c' , and c'' . By “constants,” we mean that these terms do not depend on $\Delta(p_{X|A}, \hat{f})$. The constants c , c' , and c'' depend only on p . $B(\mathcal{F}, D)$ depends on p , the model class \mathcal{F} , and dataset size D . We describe how this result can be used as a scaling law in Section 5.

Finally, we note that although our result is specific to the DGP given in Theorem 4.3, we hope it provides a template for future analyses. Even so, the DGP above is fairly general: that A is Bernoulli is without loss of generality; and $X \perp A$ does not hold in general but should not affect an analysis of Pareto-optimal classifiers. The distribution of $Y|X, A$ is only restrictive in that the contribution of A is additive and moderated by a constant ζ .

Key proof intuition. One might try to obtain the PF by solving the constrained minimization $\hat{f}_{\underline{\Delta}} = \arg \min_{f \in \mathcal{F}} \mathcal{L}(p_{X,A,Y}, f)$ subject to $\Delta(p_{X,A,Y}, f) = \underline{\Delta}$, then computing $\mathcal{L}(p_{X,A,Y}, \hat{f}_{\underline{\Delta}})$ for all $\underline{\Delta}$. However, this problem is highly difficult to solve analytically and generally requires strong assumptions on the model class \mathcal{F} . Alternatively, one may wish to iterate over all possible \hat{f} and compute their corresponding loss and fairness gap values (akin to [10, 24]), but this approach is only feasible for finite-dimensional, categorical features where the number of possible classifiers is small [40]; this approach does not scale for large models with high-dimensional, unstructured inputs.

To address these issues, we use a technique that often motivates in-processing methods and fair representation learning [35, 21, 15]: that one can induce a fairness gap $\underline{\Delta}$ by constructing an *artificial train distribution* $q \neq p$. In other words, we can transform the constrained minimization problem $\min_{f \in \mathcal{F}} \mathcal{L}(p_{X,A,Y}, f)$ subject to $\Delta(p_{X,A,Y}, f) = \underline{\Delta}$ into an unconstrained problem $\min_{f \in \mathcal{F}} \mathcal{L}(q_{X,A,Y}, f)$, where q “tilts” p so that the solution \hat{f} to the latter problem has the desired fairness gap $\Delta(p_{X,A,Y}, \hat{f}) = \underline{\Delta}$. Note that “tilting” q does *not* have any bearing on what distribution the developer actually uses to train their model— q is an abstraction.¹⁴ To provide further intuition, recall that there is a known equivalence between minimizing an objective function subject to a constraint and minimizing the Lagrangian. Our approach leverages another notion of duality where minimizing $\mathbb{E}_p[\text{loss}]$ subject to a fairness constraint is equivalent to minimizing $\mathbb{E}_q[\text{loss}]$ for some q .

This change of measure allows us to characterize a Pareto-optimal classifier \hat{f} for a given fairness gap $\underline{\Delta}$ in terms of the Bayes optimal classifier $q(1|x, a)$ for the q used to induce $\underline{\Delta}$. Then, we apply Theorem 4.1, where Theorem 4.2 maps to the condition on S in Theorem 4.1. In summary, our approach alleviates the two challenges described above: for (i), we use the Bayes optimal classifier on the effective train distribution q to simulate the constrained loss-minimization problem that is difficult to solve analytically; for (ii), we avoid imposing strong assumptions on the model class \mathcal{F} by using a milder model symmetry assumption.

5 Applying the Scaling Law to the LDA Requirement

Theorem 4.3 can be viewed as a scaling law. Indeed, it provides a closed-form expression for the loss-fairness Pareto frontier (PF) that involves three constants that do not depend on \mathcal{F} and D , then one constant $B(\mathcal{F}, D)$ that does. This implies that finding the PF for a large model class \mathcal{F}^+ and

¹⁴We further emphasize that, although this discussion seems to suggest that we are restricting the allowable train distribution, that is not the case. We are simply imposing an *effective* train distribution as a proof technique to analytically characterize the PF.

large dataset size D^+ involves two steps. First, fit the unknown constants using (a smaller) model class \mathcal{F}^- and a (smaller) dataset size D^- . Second, given an understanding of how $B(\mathcal{F}, D)$ changes with \mathcal{F} and D , one can plug \mathcal{F}^+ and D^+ into $B(\mathcal{F}^+, D^+)$ to extrapolate the PF for \mathcal{F}^+ and D^+ . Luckily, past works provide a template for the form of B ; specifically, previous works such as [32, 7] show that the minimum loss scales with $\Theta(1/N^\alpha + 1/D^\beta)$ for some $\alpha, \beta > 0$. Because B is a linearly additive constant in Theorem 4.3, this implies that B also scales at the same rate.

Before presenting the procedure in detail, we note that the existence of a closed-form expression for the PF does *not* mean that all loss-fairness PFs look the same. In fact, the shape of the PF can vary significantly depending on the values of the constants, as we show in Section 6.1 (Figures 3 to 5). The constants are *context-dependent*, and thus the shape of the PF is also *context-dependent*.

Procedure. Given training data, test data, and a compute budget as well as an estimate of N^+ and D^+ , as described in Section 3, a claimant would apply the scaling law as follows:

1. Given a small model class N^- and small training dataset D^- , empirically trace out the loss-fairness PF for N^- and D^- . To do so, train a set of models, each of which is obtained by minimizing the BCE loss on D^- plus a regularizer that encourages demographic parity. Varying the weight on the regularizer induces different fairness gaps. For each trained model, compute its loss and fairness gap on the given test data. Thus, each model marks a point on the loss vs. fairness gap plane. The lower convex hull of these points forms the empirical PF. The number of trained models as well as N^- and D^- should be chosen based on one's compute budget.
2. Repeat this for different values of N^- and D^- , as permitted by one's compute budget.
3. Using these experiments, fit the constants C_1 through C_7 to each empirical PF using the following scaling law:

$$\begin{aligned} \text{loss}(\underline{\Delta}) = & C_1 + C_2/(N^-)^{C_3} + C_2/(D^-)^{C_4} \\ & - C_5 \cdot C_6 \log(1 - C_7 + \underline{\Delta}) - C_5 \cdot (1 - C_6) \log(C_7 - \underline{\Delta}) \\ & + (C_7 - \underline{\Delta})(1 - C_7 + \underline{\Delta}) \left(\frac{C_5 \cdot C_6}{2(1 - C_7 + \underline{\Delta})^2} + \frac{C_5 \cdot (1 - C_6)}{2(C_7 - \underline{\Delta})^2} \right), \end{aligned}$$

with appropriate values for N^- and D^- . Note that C_3 and C_4 are often set to 0.5 [32, 7].

4. Once estimates of C_1 through C_7 have been obtained, one can extrapolate the PF for the contested model by using the same functional form as above, except substituting N^+ and D^+ for N^- and D^- .
5. Alternatively, if one is given a specific loss-fairness pair $(\text{loss}(\underline{\Delta}), \underline{\Delta})$, one can use the functional form above to determine the values of N^+ and D^+ such that $(\text{loss}(\underline{\Delta}), \underline{\Delta})$ lies on the PF. This would tell the claimant how many resources the defendant needs to achieve that pair of values.¹⁵

Given that there are only 7 constants to fit, one could fit the scaling law by training as few as 7 small, high-quality models. In practice, the more models, the better (see discussion of Step 1 below).

Note on implementation. We note that our approach “fails gracefully” in that it is *conservative*: if a claimant finds the contested model is δ -far from the PF, then it is *at least* that far. There are two reasons why our approach is conservative. First, the empirical PF is always conservative by definition; there may be (and almost always are) models that Pareto dominate the models one finds empirically. Second, the expression in Theorem 4.3 is an inequality; it gives an upper bound on the loss of a Pareto-optimal model for a given fairness gap.

Considerations for Step 1. There are multiple ways to trace out the PF empirically. For example, what we describe above is known as linear scalarization. Many works explore other methods (cf. Section 7). There are two main ways that the choice of method affects the claimant's results: (1) some methods are better at finding *Pareto-optimal* models across a wide range of fairness gaps, and (2) some methods find them more *efficiently* without having to train many models. Thus, a good method

¹⁵Returning to Section 3, this analysis relies on the mild assumption that the PF improves monotonically as N and D increase. By our result (Theorem 4.3), this holds true because $B(\mathcal{F}, D)$, which is the only term that depends on the model class and dataset size, decreases as N and D increase.

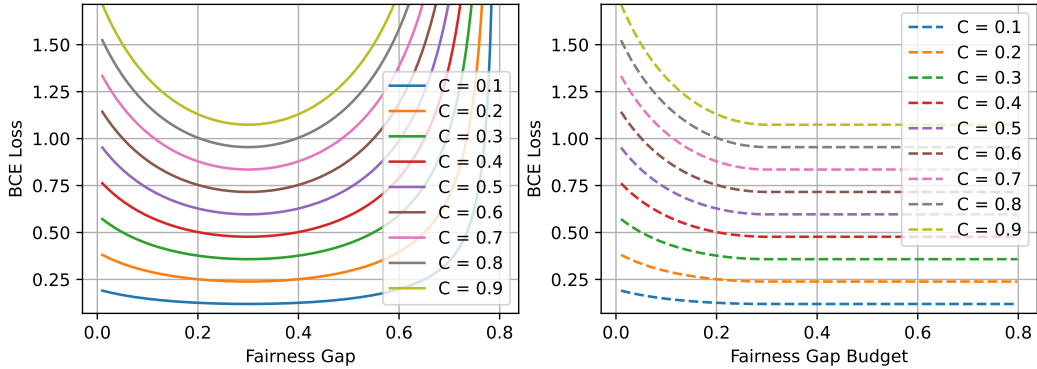


Figure 3: Simulations showing the shape of the closed-form expression for the Pareto frontier given in Theorem 4.3 for fixed values of $c' = 0.5$ and $c'' = 0.8$ while varying c . The left plot shows the precise closed-form, which is the lowest achievable loss among classifiers that have *exactly* the fairness gap value on the x-axis. The right plot shows lowest achievable loss among classifiers that satisfy the fairness gap *budget* on the x-axis.

will help the claimant get as close to the true PF as possible (which can only help the claimant increase the gap between the contested model and the PF and thus strengthen their case) while training as few models as possible (and thus using as few resources as possible). Our scaling law is plug-and-play: as the methods for finding Pareto-optimal models efficiently improve, so too does our procedure.

Considerations for Step 2. Although not strictly necessary, re-running Step 1 on different values of N^- and D^- will generally improve the estimates of C_1 through C_7 . There is a trade-off here: for a fixed compute budget, one can either run Step 1 multiple times with different (N^-, D^-) values, or run it once with a N^- and D^- that are as close to N^+ and D^+ as possible. One should plan accordingly based on one's compute budget.

Considerations for Step 3. One may find that there are multiple sets of constants that fit the empirical PF well, as we explore in Section 6 and Appendix E. One could choose the set of constants that minimize the distance between the empirical PF and the fitted PF. Unintuitively, this might not be the appropriate choice. Recalling that the PF marks the lowest loss for each fairness gap, no observed point can lie below the true PF. Thus, one may wish to use the PF that is as close to the empirical one as possible while lying entirely below it.

Finally, we note that letting B scale with $N^{-\alpha} + D^{-\beta}$ is well supported by previous works on large models (language models, in particular). As discussed in Section 1, our work is intended for large models, as this is where the LDA requirement imposes the greatest burden. One may wish to adjust the form for B as appropriate.

6 Experiments

In this section, we run experiments on synthetic data to test our main result, Theorem 4.3, and stress test its assumptions. Our experiments also demonstrate how one might apply Theorem 4.3 in practice.

6.1 Results #1: Visualizing the closed-form Pareto frontier

We begin by visualizing the behavior of the (4). Recall that (4) expresses loss as a function of the fairness gap Δ , where there are four constants: B , c , c' , and c'' . In Figures 3 to 5, we show how the shape of (4) changes for different values of each constant, while keeping the other constants fixed and letting $B, \varepsilon = 0$. We provide further figures in Appendix E.

On the left, we plot the theoretically predicted Pareto frontier (PF) that is traced out by finding the lowest-loss classifier for an *exact* fairness gap Δ . Specifically, we evaluate the expression in

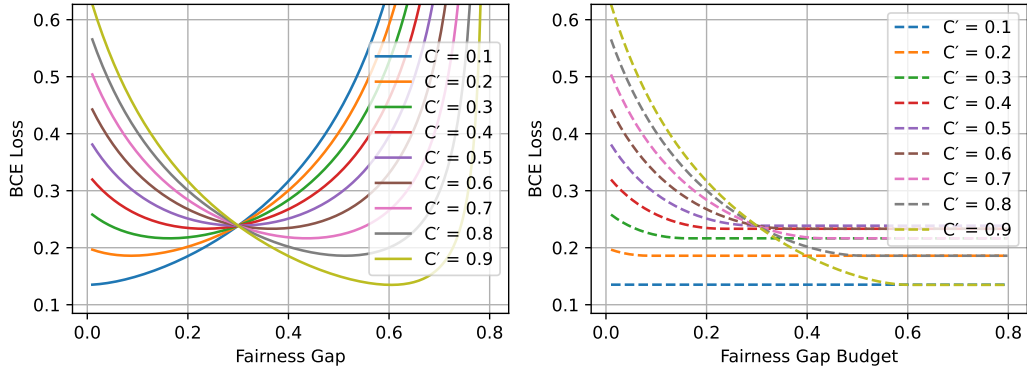


Figure 4: Simulations showing the shape of the closed-form expression for the Pareto frontier given in Theorem 4.3 for fixed values of $c = 0.2$ and $c'' = 0.8$ while varying c' . The left plot shows the precise closed-form, which is the lowest achievable loss among classifiers that have *exactly* the fairness gap value on the x-axis. The right plot shows lowest achievable loss among classifiers that satisfy the fairness gap *budget* on the x-axis.

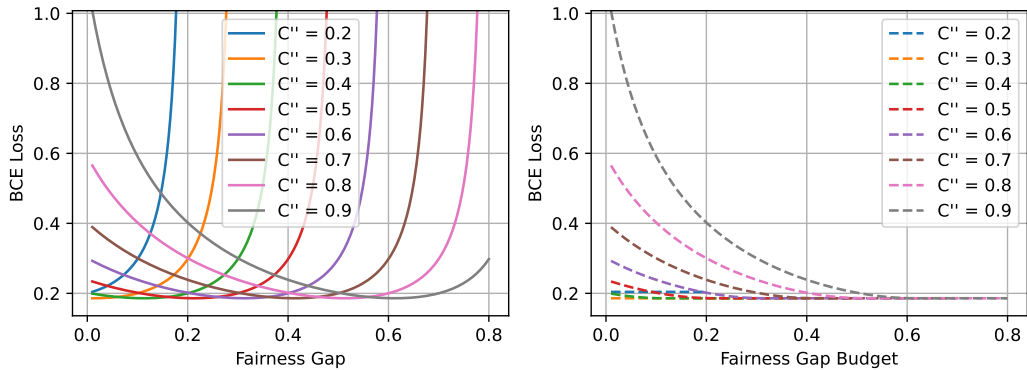


Figure 5: Simulations showing the shape of the closed-form expression for the Pareto frontier given in Theorem 4.3 for fixed values of $c = 0.2$ and $c' = 0.8$ while varying c'' . The left plot shows the precise closed-form, which is the lowest achievable loss among classifiers that have *exactly* the fairness gap value on the x-axis. The right plot shows lowest achievable loss among classifiers that satisfy the fairness gap *budget* on the x-axis.

Theorem 4.3, disregarding ε , over a range of Δ values (typically from 0 to 1). As one might expect, the loss decreases as Δ increases, then increases when a model is forced to have large fairness gap Δ .

To visualize the lowest loss achievable at or below a given fairness gap *budget* (rather than a fairness gap), we repeat the same simulation as in the left plot, then take the minimum loss value to the left of and including the current x-value (i.e., of the current fairness gap). Therefore, compared to the plot on the left, the plot on the right is, by definition, non-increasing. Intuitively, this gives the typical form of the PF by plotting the lowest achievable loss among classifiers with fairness gaps at or below the fairness gap budget given by the *x*-value.

We observe that increasing c shifts the PF upwards while also increasing its curvature; changing c' tilts the PF; and increasing c'' moves the PF to the right.

6.2 Results #2: Experiments on synthetic data demonstrating scaling law

We also provide a set of experiments on synthetic data, designed to probe the robustness of our theoretical result and demonstrate how the scaling law would be applied. We find that the PFs

predicted by our theory closely matches the empirical PFs, validating our scaling law approach to assessing the existence of a less discriminatory model (LDA).

These experiments allow us to manipulate key aspects of the data generating process and training setup to evaluate how well the assumptions and predictions of our theory hold up in practice. These experiments stress test the conditions of Theorem 4.3 in three critical ways:

1. We relax the assumption on the data generating process in Theorem 4.3 so that $X \not\perp A$.
2. Recall that one of our main proof techniques is to transform the constrained minimization problem into an unconstrained one by creating an artificial train distribution q (that does not actually exist). Doing so allows us to “tune” the fairness gap, then find the loss-minimizing model. In our experiments, we test whether this approach is representative of the true loss-minimizing models at various fairness gap values. Our experiments use a standard training procedure with a fairness regularization term and linear scalarization to trace out the PF.
3. Recall that our second proof strategy is to use a Bayes optimal estimator for an artificial distribution to approximate a Pareto-optimal model. This approach further relies on Theorem 4.2. We test this approach and the corresponding assumption in our experiments. We trace out the empirical PF by training a collection of models on the synthetic train data, using the lower convex hull of the resulting (loss, fairness) characteristics as the empirical PF. Thus, our experiments test whether the approach we take to derive our analytic result holds empirically.

In short, our experiments stress test our theoretical result by relaxing a condition on the data generating process and checking whether our main assumption and proof techniques hold in practice.

Synthetic data generation. We generated a synthetic dataset with 10,000 samples, where each sample is a 20-dimensional vector with binary group labels. Each x is sampled i.i.d. from a standard isotropic multivariate Gaussian distribution. The group label $a \in \{0, 1\}$ is deterministically assigned by linearly projecting the first two dimensions of x onto a scalar, then thresholding, where the linear weights and bias are randomly sampled from a multivariate Gaussian, and the threshold is chosen so that a fixed fraction of the population belongs to Group 1 (i.e., $p(A = 1)$ is the desired value). Because A depends on X , they are not independent, as required in Theorem 4.3; our experiments therefore test whether the closed-form PF holds despite this relaxation.

The target variable $y \in \{0, 1\}$ is sampled from a Bernoulli distribution with probability $\mathbb{P}(Y = 1 | X, A) = \sigma(g(X) - \zeta A)$, where $g : \mathbb{R}^{20} \rightarrow \mathbb{R}$ is a fixed, randomly initialized 2-layer MLP with a hidden layer of size 32 applied to X , $\zeta \geq 0$, and $\sigma(\cdot)$ denotes the sigmoid function. It thus mirrors the data generating process in Theorem 4.3, except that X and A are not independent. We show results for various values of ζ . Finally, our experiments use the same distribution for the train and test sets.

Obtaining the empirical PF. We obtain the empirical PF by training models with varying loss-fairness characteristics. To do so, we use linear scalarization, i.e., we set the loss to be the sum of the BCE loss and the fairness gap $\mathcal{L}_{\text{total}} = \mathcal{L}_{\text{BCE}} + \lambda \cdot \mathcal{L}_{\text{DP}}$ and vary λ . As discussed at the end of Section 5, there are many methods for surfacing Pareto-optimal models across a wide range of fairness gap values; the better the method, the more accurate the empirical PF. We use linear scalarization, as it is a popular and simple method.

As in our theoretical result, we use demographic parity as our fairness notion. We vary λ across 100 values between -3 and 5, with a higher density of values in the -3 to 0 portion.¹⁶ For every scalarization value, we run 3 trials, then trace out the empirical PF (with mild smoothing and averaging). Further training details are given in Appendix E. Note that there are more advanced methods for obtaining the empirical PF than linear scalarization; the better the method is at finding Pareto-optimal models, (i) the fewer models need to be trained to obtain the PF, and (ii) the more accurate the PF.

To get the empirical PF, we compute each trained model’s BCE loss and fairness gap on the held-out test data. We plot these (loss, fairness) pairs on the BCE loss vs. demographic parity gap plane. To trace the empirical PF (the lowest achieved loss for each given demographic parity gap), we connect the points forming the lower convex hull of the points.

¹⁶Although λ ’s are usually positive, we use negative values to test whether the PF curves upward for large fairness gaps as predicted by our theory.

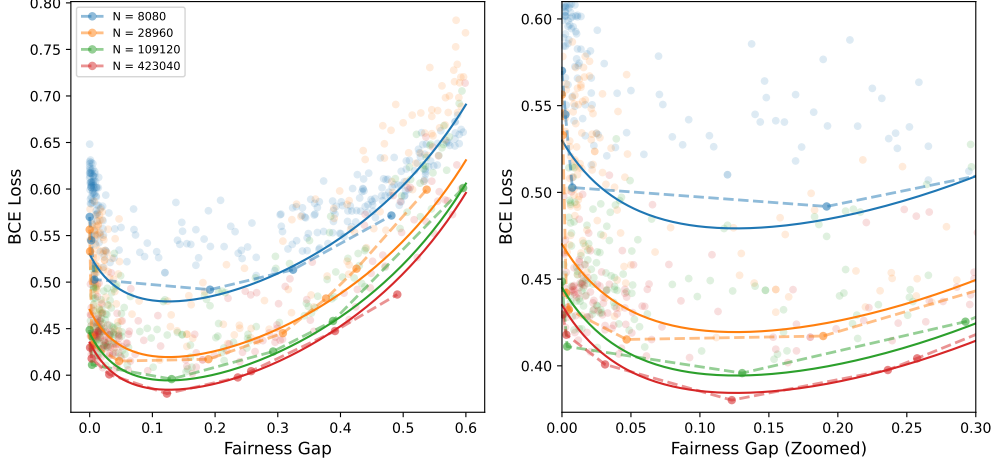


Figure 6: Pareto frontier for different model sizes under $(\pi = 0.2)$ and bias strength $\zeta = 0.5$. Each point corresponds to a trained model with a different fairness regularization weight λ . The dashed lines show the empirical Pareto frontier, created by finding the lower convex hull of all the points. The solid lines show fitted curves to the points on the Pareto frontier using Theorem 4.3 with $c = 0.0176$, $c' = 0.92$, $c'' = 0.1424$, with bias -0.285 , loss scaling law $55(N^{-0.7} + D^{-0.5})$. The left panel shows the frontier across the range of Δ , while the right panel zooms in on $\Delta \in [0, 0.3]$. The fitted curve mimics the empirical data well though it is imperfect. We found that there were many possible fits, depending on the precise choice. We show another possible fit in Figure 11 below.

Testing the scaling law. To test whether the scaling law holds, we demonstrate that there is a fixed of constants C_1 through C_7 such that the closed-form expression given in Theorem 4.3 predicts the PF across different values of N and D , as laid out in Section 5. We focus on the effect of model scaling, leaving D constant and only varying the model size N . We then use the procedure described in Section 5 to “scale” the curve. *If the empirical PFs are close to the predicted curves, it would validate our method: that training small models can be used to approximate the PF of larger models.* In Figure 6 and similar plots in Appendix E, the dashed lines give the empirical PFs, and the solid lines give the ones predicted by our theory.

Results. Our findings corroborate our theoretical result: First, from the y-intercepts alone, we verify that $B(\mathcal{F}, D)$ nearly perfectly scales proportionally to $N^{-\alpha} + D^{-\beta}$ plus an additive constant, as predicted. Second, the empirical PFs follow the shape as our closed-form scaling law. Even small changes to the expression in Theorem 4.3 would not yield a similarly good fit. Perhaps somewhat surprisingly, our theory predicts that the effect of scaling via B is linearly additive, and our experiments validate this prediction. Both of these findings provide strong evidence supporting: (i) our Theorem 4.2 and (ii) the use of Bayes optimal estimators on artificially constructed train distributions to approximate Pareto-optimal models (which allows us to obtain our result with minimal assumptions on the model class and for unstructured inputs).

We note that the fitted curve mimics the empirical data well though imperfectly, which may occur for several reasons. The first is that the empirical PF is always imperfect since finding Pareto-optimal models is difficult, e.g., due to factors discussed in Section 5 under “Considerations for Step 1.” The second is that (4) is an upper bound—therefore, there is a possibility that the shape of the true PF differs slightly from the predicted one (though our result is, in some sense, tight as seen in Appendix D). The third is that there are many possible fits for the same empirical PF, as we show in Appendix E. In practice, one may choose to fit the curve as closely as possible to the data or, noting that the PF is an idealized concept, fit the curve to lower bound the empirical points.

7 Background and Related Work

AI audits. The study of AI audits has grown rapidly in the past few years [50, 44, 25, 51]. Although the range of methods and objectives for audits varies greatly, many agree that audits serve an important function in AI accountability, whether conducted by civil society groups, private actors, or regulators

[14, 38, 48]. Broadly defined, AI audits refer to the class of methods by which AI systems are evaluated and tested. Audits can, for instance, be used to assess compliance with the law or to test a model’s performance with respect to the model developer’s claims.

Researchers have identified multiple challenges to conducting AI audits [25], including the limited access granted to third-party auditors [57, 17, 16], conflicts of interest that can arise due to financial ties between auditors and auditees [20, 59], poor researcher protections [42], and difficulties in verifying the veracity of self-reported information [58, 22, 60]. Among these issues, our work seeks to address the difficulties of producing (convincing) evidence in resource-, data-, and information-constrained settings. Specifically, the auditor (or claimant) is often at a disadvantage when producing evidence that surpasses the relevant (context-dependent) standard in that (i) they typically possess fewer resources than the other party (e.g., model developer), (ii) they have limited if any access to the system they seek to audit, and (iii) they may lack technical expertise or domain knowledge.

Disparate impact doctrine. In the US, disparate impact is a legal doctrine used to demonstrate that a facially neutral practice or practice discriminates against a protected group by showing that it has a disproportionately negative impact on them, even if there is no intent to discriminate [12]. It is often contrasted with disparate treatment, which concerns intentional discrimination [8]. Under disparate impact doctrine, plaintiffs typically show that a practice has disparate impact by providing statistical evidence. This doctrine was one of the main drivers behind the field of algorithmic fairness and the development of outcome-based fairness metrics [27]. Such fairness metrics generally study classification, e.g., decisions to interview or not, hire or not, promote or not. For example, one way to measure quantify discrimination is to compare the rates at which different groups are selected (interviewed, hired, promoted), often referred to as “selection rates.” The absolute difference in selection rates is often referred to as the “demographic parity gap.”

From a legal perspective, there is precedent for assessing disparate impact using a guideline known as the Four-Fifths Rule, which states that a practice has disparate impact if the selection rate for a protected group is less than four-fifths of the selection rate for the group with the highest rate. Although the use of selection rates to assess discrimination is highly debated (as are fairness metrics, more broadly), selection rates are often used in disparate impact analyses because they provide a simple and intuitive way to compare group outcomes that does not suffer from a selection bias problem (that makes the estimation of true positive and false positive rates difficult). Selection rates remain a popular choice in practice, e.g., see NYC’s Local Law 144 of 2021.

Less discriminatory alternatives (LDAs). The LDA requirement arose in US anti-discrimination law, as described further in Section 2. It has become a critical part of disparate impact doctrine following the landmark *Griggs v. Duke Power Co.* decision in which the Supreme Court held that discrimination can occur even in the absence of intent (i.e., facially neutral practices can also be discriminatory) [12]. Within disparate impact doctrine, the LDA requirement urges decision makers to consider less harmful alternatives among equally effective options as a structural way to assess and remove unnecessary discrimination [9]. We refer readers to Lamber [39], not [1], Rutherglen [54] for further analyses of the role of LDAs in disparate impact claims.

Several scholars critically examine the efficacy of disparate impact doctrine and practical application of the LDA requirement. Many observe that identifying precise and legally sufficient LDAs is difficult for plaintiffs [1, 55], and others highlight the inconsistent (and sometimes deferential) application of the business necessity standard by courts that can undermine LDA-based claims [26]. Some factors even discourage employers from seeking less discriminatory alternatives, including the risk of reverse discrimination lawsuits and legal uncertainty following *Ricci v. DeStefano* [28, 29]. Together, these critiques reveal a gap between the aspirations of disparate impact theory and the practical barriers faced by litigants. Our work takes the following perspective: while the LDA requirement remains intact, claimants increasingly need methods to demonstrate the existence of feasible alternatives.

Less discriminatory algorithms. Recent works examine the LDA requirement as it applies to algorithmic decision-making. Gillis et al. [24] cast the search for LDAs as an mixed integer program, then directly search for an algorithm that minimizes error rate disparity subject to performance criteria. Laufer et al. [40] provide theoretical insights showing, among other takeaways, that identifying the least discriminatory alternative is NP-hard and may only constitute an LDA for the distribution or data over which it was derived. Our work mirrors the motivation of Gillis et al. [24] in that we seek to provide an operationalizable method for plaintiffs. However, as both Gillis et al. [24] and Laufer et al. [40] note, producing an LDA is computationally expensive and thus existing approaches do not

scale to for large models, which are increasingly important to audit. Our work adds to this space by providing a tool for plaintiffs with limited compute and data.

From a legal perspective, Black et al. [11] argue that defendants should be required to conduct a reasonable search for LDAs before deployment, in large part due to the resource asymmetry we discuss. Until new legal requirement compelling such a search arises, our approach helps provide tooling for claimants to prove the existence of a reasonable LDA with limited resources. Furthermore, we believe that even if the burden were to shift, claimants should still be equipped to independently verify that a feasible LDA does not exist rather than trust the developer’s claims.

Performance-fairness Pareto frontiers (PFs). In many settings a trade-off between fairness and performance emerges [10, 43, 37]. In such cases, the performance-fairness PF characterizes the best fairness and performance that can be simultaneously achieved (i.e., the best performance than can be achieved for a given fairness level, or vice versa). Various works propose methods for improving Pareto optimality or tracing out the performance-fairness PF, including Navon et al. [47], Ruchte and Grabocka [53], Singh et al. [56], Rothblum and Yona [52], Kamani et al. [34], Liu and Vicente [41], Chzhen and Schreuder [19], Zeng et al. [62]. In many of these works, the goal is to develop efficient methods for tracing out the PF, but they still assume the resources needed to train *at least* one model. In our work, we seek to improve scalability in a different sense: one can trace out the PF in small-model, low-data regimes and extrapolate the PF to large-model, large-data regimes (and thus one does not even need the resources required to train a large model). To the best of our knowledge, none of the existing works provide closed-form expressions for the fairness PF.

Scaling laws. Scaling laws have been widely studied in the context of deep learning, typically used to predict how model behavior improves with increasing model size, data, and compute [31, 36, 32, 7]. In this work, we seek to provide a theoretically-grounded scaling law for the loss-fairness PF that allows one to fit the PF with small models and small datasets, then extrapolate to larger models and datasets with the help of the power law (that applies to loss) found in the works above.

8 Conclusion, Limitations, and Future Work

In this work, we tackle the problem of resource-information asymmetry in AI audits and legal cases involving AI. We focus our discussion on Title VII’s “less discriminatory alternative” (LDA) requirement as a case study exhibiting how claimants often face a steep uphill battle in order to meet their evidentiary burden (as noted in previous works [11, 24, 40]). We are motivated by this issue to develop tools and methods to reduce the hurdles claimants face. Our main contributions are (1) to cast the problem of finding an LDA as one of estimating the performance-fairness Pareto frontier (PF), (2) to provide a novel technical result that, to our knowledge, provides a first closed-form expression for the performance-fairness PF, and (3) to show how this result can be used as a scaling law for performance-fairness PFs that directly addresses both the resource and information asymmetry issues posed by the LDA requirement.

Next, we identify the assumptions (both technical and conceptual) of our work, which highlight potential limitations and avenues for future work:

1. Our theoretical analysis is conducted for specific notions of fairness and performance. We justify these choices in Section 3 and Section 7, and we believe that future work tackling other definitions would be valuable. Our work also relies on disparate impact and business necessity being measurable; we do not preclude the use of multiple metrics to measure fairness or performance, and studying the more complex multi-objective optimization problem in which there are more than two metrics of interest would be compelling future work. We are unsure how to address settings in which fairness and performance are not measurable, and we welcome future work that explores the LDA requirement in such settings (e.g., when fairness is ordinal).
2. Our result applies for the DGP given in Section 4.2. A compelling direction for future work would be to determine how well our result holds, for real data and *even* for other DGPs. Although stylized, the DGP we study still allows for significant generality. We also recommend future work, both theoretical and empirical, on the form of the loss-performance PF for other DGPs.
3. Relatedly, our main proof technique that allows us to obtain an analytic expression without strong assumptions on the inputs or the model class is to use a notion of “duality” that approximates Pareto-optimal classifiers with varying fairness characteristics using Bayes optimal estimators

on artificially constructed training distributions. To do so, use ζ to “tilt” the (artificial) train distribution. As one explores other DGPs, one could also explore (i) the conditions under which this duality holds and (ii) alternative ways of tilting the training distribution.

4. Theorem 4.2 appears to hold in our experiments. Given that this assumption does not directly depend on the experimental choice of data generating process (DGP), this is strong evidence supporting it. However, we suggest two directions of exploration: (i) further theoretical work to understand when this assumption may not hold, which may result in an additional term in (4) that allows Theorem 4.2 to be removed and therefore strengthens the result; and (ii) empirical investigations to identify when this assumption breaks down in practice.
5. Our result (4) is an upper bound. Although it is tight in some sense (that it holds with equality for some g), we believe a compelling direction for future work is to identify a tighter bound.
6. As mentioned in Section 5, the form of B that we adopt is borrowed from the literature on large language models. One could explore alternative forms of B that may be more appropriate for other model classes and sizes.

We identify several other considerations and extensions:

1. A defendant may be able to argue that, in failing to produce a specific less discriminatory alternative (LDA), this approach does not pass the necessary evidentiary standard. As noted in Footnote 8, if the court does not consider this evidence strong enough to satisfy the LDA requirement, we hope that it can be used to support the plaintiff’s requests for further discovery, including data and model access that they may be initially denied.
2. Our experimental results are limited. There are several directions for future work, including conducting experiments on real datasets, further stress testing the limitations of our theoretical results, and running experiments at greater scale.
3. Our approach requires access to some training and test data. We feel that this requirement is unavoidable, and our contribution is to significantly decrease the amount of data that the claimant needs. However, we acknowledge that this requirement may still pose a hurdle and leave the exploration of techniques that further mitigate the data requirements to future work.
4. The empirical PF is, in a sense, a random variable that depends on the sampled training data and the randomness of the training procedure. One could explore the confidence intervals of the estimated PF that result from different training runs. Similarly, our theoretical result does not have a notion of uncertainty; future work could explore a high-probability version of our result.

Acknowledgments and Disclosure of Funding

We thank the research group of Percy Liang and the RegLab for their valuable feedback during the early stages of this project. This work is supported by the CSET Foundational Research Grant on audit methods for frontier models.

References

- [1] The Civil Rights Act of 1991 and Less Discriminatory Alternatives in Disparate Impact Litigation. *Harvard Law Review*, 106(7):1621–1638, 1993. URL <http://www.jstor.org/stable/1341935>.
- [2] Note, State v. Loomis: Wisconsin Supreme Court Requires Warning Before Use of Algorithmic Risk Assessments in Sentencing. *Harvard Law Review*, 130(5):1530–1537, Mar. 2017. URL https://harvardlawreview.org/wp-content/uploads/2017/03/1530-1537_online.pdf.
- [3] Cahoo v. SAS Analytics Inc., January 2019.
- [4] Bauserman v. Unemployment Insurance Agency, July 2022.
- [5] Complaint and Request for Investigation, Injunction, and Other Relief Submitted by the Electronic Privacy Information Center (EPIC), January 2024.
- [6] A. Agarwal, A. Beygelzimer, M. Dudík, J. Langford, and H. Wallach. A reductions approach to fair classification. In *International conference on machine learning*, pages 60–69. PMLR, 2018.

[7] Y. Bahri, E. Dyer, J. Kaplan, J. Lee, and U. Sharma. Explaining neural scaling laws. *Proceedings of the National Academy of Sciences*, 121(27):e2311878121, 2024.

[8] S. Barocas and A. D. Selbst. Big Data’s Disparate Impact. *California Law Review*, 104(3): 671–732, 2016. doi: 10.15779/Z38BG31. URL <https://www.cs.yale.edu/homes/jf/BarocasSelbst.pdf>.

[9] J. Bastress, Robert M. The Less Restrictive Alternative in Constitutional Adjudication: An Analysis, a Justification, and Some Criteria. *Vanderbilt Law Review*, 27(5):971–1006, 1974. URL <https://scholarship.law.vanderbilt.edu/vlr/vol27/iss5/3>.

[10] D. Bertsimas, V. F. Farias, and N. Trichakis. The price of fairness. *Operations research*, 59(1): 17–31, 2011.

[11] E. Black, L. Koepke, P. Kim, S. Barocas, and M. Hsu. The Legal Duty to Search for Less Discriminatory Algorithms. *arXiv preprint arXiv:2406.06817*, 2024.

[12] A. W. Blumrosen. Strangers in Paradise: Griggs v. Duke Power Co. and the Concept of Employment Discrimination. *Michigan Law Review*, 71(1):59–110, 1972.

[13] S. Boucheron, G. Lugosi, and P. Massart. Basic Inequalities. In *Concentration Inequalities: A Nonasymptotic Theory of Independence*. Oxford University Press, online edition edition, 2013. doi: 10.1093/acprof:oso/9780199535255.003.0002. URL <https://doi.org/10.1093/acprof:oso/9780199535255.003.0002>. Accessed: 2025-05-11.

[14] S. Brown, J. Davidovic, and A. Hasan. The algorithm audit: Scoring the algorithms that score us. *Big Data & Society*, 8(1):2053951720983865, 2021.

[15] F. P. Calmon, D. Wei, B. Vinzamuri, K. N. Ramamurthy, and K. R. Varshney. Optimized pre-processing for discrimination prevention. In *Proceedings of the 31st International Conference on Neural Information Processing Systems*, NIPS’17, pages 3995–4004, Red Hook, NY, USA, 2017. Curran Associates Inc. ISBN 9781510860964.

[16] S. Casper, C. Ezell, C. Siegmann, N. Kolt, T. L. Curtis, B. Bucknall, A. Haupt, K. Wei, J. Scheurer, M. Hobbahn, et al. Black-box access is insufficient for rigorous ai audits. In *Proceedings of the 2024 ACM Conference on Fairness, Accountability, and Transparency*, pages 2254–2272, 2024.

[17] S. H. Cen and R. Alur. From Transparency to Accountability and Back: A Discussion of Access and Evidence in AI Auditing. In *Proceedings of the 4th ACM Conference on Equity and Access in Algorithms, Mechanisms, and Optimization*, pages 1–14, 2024.

[18] A. Chouldechova. Fair prediction with disparate impact: A study of bias in recidivism prediction instruments. *Big data*, 5(2):153–163, 2017.

[19] E. Chzhen and N. Schreuder. A minimax framework for quantifying risk-fairness trade-off in regression. *The Annals of Statistics*, 50(4):2416–2442, 2022.

[20] S. Costanza-Chock, I. D. Raji, and J. Buolamwini. Who Audits the Auditors? Recommendations from a field scan of the algorithmic auditing ecosystem. In *Proceedings of the 2022 ACM Conference on Fairness, Accountability, and Transparency*, pages 1571–1583, 2022.

[21] M. Feldman, S. A. Friedler, J. Moeller, C. Scheidegger, and S. Venkatasubramanian. Certifying and Removing Disparate Impact. In *Proceedings of the 21th ACM SIGKDD International Conference on Knowledge Discovery and Data Mining*, KDD ’15, pages 259–268, New York, NY, USA, 2015. Association for Computing Machinery. ISBN 9781450336642. doi: 10.1145/2783258.2783311. URL <https://doi.org/10.1145/2783258.2783311>.

[22] O. Franzese, A. S. Shamsabadi, and H. Haddadi. OATH: Efficient and Flexible Zero-Knowledge Proofs of End-to-End ML Fairness. *arXiv preprint arXiv:2410.02777*, 2024.

[23] S. Friedler, S. Choudhary, C. Scheidegger, E. Hamilton, S. Venkatasubramanian, and D. Roth. A comparative study of fairness-enhancing interventions in machine learning. In *FAT* 2019 - Proceedings of the 2019 Conference on Fairness, Accountability, and Transparency*, FAT* 2019 - Proceedings of the 2019 Conference on Fairness, Accountability, and Transparency, pages 329–338. Association for Computing Machinery, Inc, Jan. 2019. doi: 10.1145/3287560.3287589. Publisher Copyright: © 2019 Copyright held by the owner/author(s); 2019 ACM Conference on Fairness, Accountability, and Transparency, FAT* 2019 ; Conference date: 29-01-2019 Through 31-01-2019.

[24] T. B. Gillis, V. Meursault, and B. Ustun. Operationalizing the search for less discriminatory alternatives in fair lending. In *Proceedings of the 2024 ACM Conference on Fairness, Accountability, and Transparency*, pages 377–387, 2024.

[25] E. P. Goodman and J. Trehu. Algorithmic auditing: Chasing AI accountability. *Santa Clara High Tech. LJ*, 39:289, 2022.

[26] S. S. Grover. The Business Necessity Defense in Disparate Impact Discrimination Cases. *Georgia Law Review*, 30(2):387–430, 1996.

[27] M. Hardt, E. Price, and N. Srebro. Equality of opportunity in supervised learning. In *Proceedings of the 30th International Conference on Neural Information Processing Systems*, NIPS’16, pages 3323–3331, Red Hook, NY, USA, 2016. Curran Associates Inc. ISBN 9781510838819.

[28] C. I. Harris and K. West-Faulcon. Reading Ricci: Whitening Discrimination, Racing Test Fairness. *UCLA Law Review*, 58:73–150, 2009.

[29] M. Hart. From Wards Cove to Ricci: Struggling Against the “Built-in Headwinds” of a Skeptical Court. *Wake Forest Law Review*, 46:261–278, 2011.

[30] D. Harwell. A face-scanning algorithm increasingly decides whether you deserve the job. *The Washington Post*, November 2019. URL <https://www.washingtonpost.com/technology/2019/10/22/ai-hiring-face-scanning-algorithm-increasingly-decides-whether-you-deserve-job/>.

[31] J. Hestness, S. Narang, N. Ardalani, G. Diamos, H. Jun, H. Kianinejad, M. M. A. Patwary, Y. Yang, and Y. Zhou. Deep learning scaling is predictable, empirically. *arXiv preprint arXiv:1712.00409*, 2017.

[32] J. Hoffmann, S. Borgeaud, A. Mensch, E. Buchatskaya, T. Cai, E. Rutherford, D. d. L. Casas, L. A. Hendricks, J. Welbl, A. Clark, et al. Training compute-optimal large language models. *arXiv preprint arXiv:2203.15556*, 2022.

[33] C. C. Jones. Systematizing Discrimination: AI Vendors & Title VII Enforcement. *University of Pennsylvania Law Review*, 171(1):235–265, 2022. URL https://scholarship.law.upenn.edu/penn_law_review/vol171/iss1/6/.

[34] M. M. Kamani, R. Forsati, J. Z. Wang, and M. Mahdavi. Pareto Efficient Fairness in Supervised Learning: From Extraction to Tracing. *arXiv preprint arXiv:2104.01634*, 2021. URL <https://arxiv.org/abs/2104.01634>.

[35] F. Kamiran and T. Calders. Data preprocessing techniques for classification without discrimination. *Knowl. Inf. Syst.*, 33(1):1–33, Oct. 2012. ISSN 0219-1377. doi: 10.1007/s10115-011-0463-8. URL <https://doi.org/10.1007/s10115-011-0463-8>.

[36] J. Kaplan, S. McCandlish, T. Henighan, T. B. Brown, B. Chess, R. Child, S. Gray, A. Radford, J. Wu, and D. Amodei. Scaling laws for neural language models. *arXiv preprint arXiv:2001.08361*, 2020.

[37] J. S. Kim, J. Chen, and A. Talwalkar. FACT: A diagnostic for group fairness trade-offs. In *International Conference on Machine Learning*, pages 5264–5274. PMLR, 2020.

[38] M. S. Lam, A. Pandit, C. H. Kalicki, R. Gupta, P. Sahoo, and D. Metaxa. Sociotechnical audits: Broadening the algorithm auditing lens to investigate targeted advertising. *Proceedings of the ACM on Human-Computer Interaction*, 7(CSCW2):1–37, 2023.

[39] J. C. Lamber. Alternatives to Challenged Employee Selection Criteria: The Significance of Nonstatistical Evidence in Disparate Impact Cases Under Title VII. *Wisconsin Law Review*, pages 1–58, 1985.

[40] B. Laufer, M. Raghavan, and S. Barocas. Fundamental Limits in the Search for Less Discriminatory Algorithms—and How to Avoid Them. *arXiv preprint arXiv:2412.18138*, 2024.

[41] S. Liu and L. N. Vicente. Accuracy and fairness trade-offs in machine learning: a stochastic multi-objective approach. *Computational Management Science*, 19(3):513–537, 2022. doi: 10.1007/s10287-022-00425-z. URL <https://link.springer.com/article/10.1007/s10287-022-00425-z>.

[42] S. Longpre, S. Kapoor, K. Klyman, A. Ramaswami, R. Bommasani, B. Blili-Hamelin, Y. Huang, A. Skowron, Z.-X. Yong, S. Kotha, et al. A safe harbor for AI evaluation and red teaming. *arXiv preprint arXiv:2403.04893*, 2024.

[43] A. K. Menon and R. C. Williamson. The cost of fairness in binary classification. In S. A. Friedler and C. Wilson, editors, *Proceedings of the 1st Conference on Fairness, Accountability and Transparency*, volume 81 of *Proceedings of Machine Learning Research*, pages 107–118. PMLR, 23–24 Feb 2018.

[44] D. Metaxa, J. S. Park, R. E. Robertson, K. Karahalios, C. Wilson, J. Hancock, C. Sandvig, et al. Auditing algorithms: Understanding algorithmic systems from the outside in. *Foundations and Trends® in Human–Computer Interaction*, 14(4):272–344, 2021.

[45] National Association of Insurance Commissioners. Insurance topics: Big data. <https://content.naic.org/insurance-topics/big-data>.

[46] National Association of Insurance Commissioners (NAIC). 2023 Life Artificial Intelligence/Machine Learning Survey Report, December 2023.

[47] A. Navon, A. Shamsian, G. Chechik, and E. Fetaya. Learning the pareto front with hypernetworks. *arXiv preprint arXiv:2010.04104*, 2020.

[48] V. Ojewale, R. Steed, B. Vecchione, A. Birhane, and I. D. Raji. Towards AI accountability infrastructure: Gaps and opportunities in AI audit tooling. In *Proceedings of the 2025 CHI Conference on Human Factors in Computing Systems*, pages 1–29, 2025.

[49] D. Ozkul. Automating Immigration and Asylum: The Uses of New Technologies in Migration and Asylum Governance in Europe. Research report (algorithmic fairness for asylum seekers and refugees project), Refugee Studies Centre, University of Oxford, 2023. URL https://www.rsc.ox.ac.uk/files/files-1/automating-immigration-and-asylum_afar_9-1-23.pdf.

[50] I. D. Raji, A. Smart, R. N. White, M. Mitchell, T. Gebru, B. Hutchinson, J. Smith-Loud, D. Theron, and P. Barnes. Closing the AI accountability gap: Defining an end-to-end framework for internal algorithmic auditing. In *Proceedings of the 2020 conference on fairness, accountability, and transparency*, pages 33–44, 2020.

[51] I. D. Raji, P. Xu, C. Honigsberg, and D. Ho. Outsider oversight: Designing a third party audit ecosystem for ai governance. In *Proceedings of the 2022 AAAI/ACM Conference on AI, Ethics, and Society*, pages 557–571, 2022.

[52] G. N. Rothblum and G. Yona. Consider the Alternatives: Navigating Fairness-Accuracy Tradeoffs via Disqualification. *arXiv preprint arXiv:2110.00813*, 2021.

[53] M. Ruchte and J. Grabocka. Scalable pareto front approximation for deep multi-objective learning. In *2021 IEEE international conference on data mining (ICDM)*, pages 1306–1311. IEEE, 2021.

[54] G. Rutherglen. Disparate Impact, Discrimination, and the Essentially Contested Concept of Equality. *Fordham Law Review*, 74(4):2313–2338, 2006.

[55] M. Selmi. Was the Disparate Impact Theory a Mistake? *UCLA Law Review*, 53:701–782, 2006.

- [56] G. Singh, S. Gupta, M. Lease, and C. Dawson. A Hybrid 2-stage Neural Optimization for Pareto Front Extraction. *arXiv preprint arXiv:2101.11684*, 2021.
- [57] I. Solaiman. The gradient of generative AI release: Methods and considerations. In *Proceedings of the 2023 ACM conference on fairness, accountability, and transparency*, pages 111–122, 2023.
- [58] G. Tang, W. Tan, and M. Cai. Privacy-preserving and trustless verifiable fairness audit of machine learning models. *International Journal of Advanced Computer Science and Applications*, 14(2), 2023.
- [59] P. Terzis, M. Veale, and N. Gaumann. Law and the Emerging Political Economy of Algorithmic Audits. In *Proceedings of the 2024 ACM Conference on Fairness, Accountability, and Transparency*, pages 1255–1267, 2024.
- [60] S. Waiwitlikhit, I. Stoica, Y. Sun, T. Hashimoto, and D. Kang. Trustless audits without revealing data or models. *arXiv preprint arXiv:2404.04500*, 2024.
- [61] M. B. Zafar, I. Valera, M. G. Rogriguez, and K. P. Gummadi. Fairness constraints: Mechanisms for fair classification. In *Artificial intelligence and statistics*, pages 962–970. PMLR, 2017.
- [62] X. Zeng, G. Cheng, and E. Dobriban. Bayes-optimal fair classification with linear disparity constraints via pre-, in-, and post-processing. *arXiv preprint arXiv:2402.02817*, 2024.
- [63] I. Zliobaite. A survey on measuring indirect discrimination in machine learning. *CoRR*, abs/1511.00148, 2015. URL <http://arxiv.org/abs/1511.00148>.

A LDAs Beyond Employment Law

The “less ___ alternative” requirement expands beyond employment to areas including housing, lending, disability, and even environmental justice. The Department of Housing and Urban Development (HUD) has a 2023 rule returning to the 2013 Fair Housing Act standard under which actuarially sound housing-insurance policies are unlawful if an equally effective, less discriminatory practice is available. The Consumer Financial Protection Bureau’s (CFPB) 2023 Fair Lending Report requires lenders to proactively search their credit-scoring models for LDAs even in the absence of litigation. A closely related duty appears in disability law; Equal Employment Opportunity Commission (EEOC) guidance under the American Disabilities Act (ADA) obliges employers to adopt any “reasonable accommodation” that meets business needs without exclusion, effectively functioning as an LDA requirement. In environmental justice, permits to proposed projects may be denied if a less harmful to human health and the environment exists (an “environmentally preferable alternative”) under National Environmental Policy Act (NEPA).

Beyond the US, comparable concepts exist. The EU employs the principle of proportionality in discrimination cases, requiring that measures be appropriate and necessary, but also that the respondent show “there is no practicable alternative.” One may argue that the LDA requirement parallels the EU’s “data minimisation” requirements under the General Data Protection Regulation (GDPR), requiring data processing to be “limited to what is necessary.” In Canada, the *Meiorin* test examines whether the employer has accommodated affected groups to the point of undue hardship. South Africa, drawing from Section 36 of its Constitution, applies a limitations analysis that considers whether less restrictive means could achieve policy objectives without discriminatory impacts.

B Helpful Lemmas

Lemma B.1. *Let μ and ν be finite probability measures of the same mass on a space \mathcal{Z} such that μ is absolutely continuous with respect to ν , i.e., $\mu \ll \nu$. Let $t(z) := \frac{d\mu}{d\nu}(z)$ denote the corresponding Radon-Nikodým derivative and $R(z) := t(z) - 1$. Let $S : \mathcal{Z} \rightarrow \mathbb{R}$ be absolutely integrable with respect to μ and ν . Then,*

$$\text{Cov}_\nu(R, S) = 0 \iff \mathbb{E}_\nu[RS] = \mathbb{E}_\nu[R]\mathbb{E}_\nu[S] \iff \mathbb{E}_\mu[S] = \mathbb{E}_\nu[S].$$

Proof. First, since μ and ν are probability measures and t is the Radon-Nikodým derivative,

$$\mathbb{E}_\nu[R] = \mathbb{E}_\nu[t - 1] = \mathbb{E}_\nu[t] - 1 = 0.$$

Furthermore, by the definition of R ,

$$\mathbb{E}_\nu[RS] = \mathbb{E}_\nu[(t - 1)S] = \mathbb{E}_\nu[tS] - \mathbb{E}_\nu[S] = \mathbb{E}_\mu[S] - \mathbb{E}_\nu[S].$$

Therefore,

$$\mathbb{E}_\mu[S] = \mathbb{E}_\nu[S] \iff \mathbb{E}_\nu[RS] = 0 = \mathbb{E}_\nu[R]\mathbb{E}_\nu[S],$$

where the last equality is a consequence of having established that $\mathbb{E}_\nu[R] = 0$. This completes the proof, with the first \iff in the lemma statement following from the definition of covariance. \square

Lemma B.2. *Consider the setup in Section 3, notation in Section 4, and data generating process in Theorem 4.3. Then,*

$$\text{Cov}_{p_{X|A=1}}(p(1 | X, A = 1), q(1 | X, A = 1)) \geq 0.$$

Proof. The covariance is well-defined since $p(1 | X, 1)$ and $q(1 | X, 1)$ have finite second moments by definition of p and q . To show that the expression is non-negative, we appeal to Chebyshev’s Association Inequality (see, e.g., [13, Theorem 2.14]), which states that if f and h are real-valued functions that are monotonic in the same direction and Z is a real-valued random variable, then $\mathbb{E}[f(Z)h(Z)] \geq \mathbb{E}[f(Z)]\mathbb{E}[h(Z)]$. Thus, $\text{Cov}(i(Z), j(Z)) = \mathbb{E}[i(Z)j(Z)] - \mathbb{E}[i(Z)]\mathbb{E}[j(Z)] \geq 0$.

To get the final result, we map Z , f , and h to quantities in our setup. Let the expectations be taken over $p(X|A = 1)$, let $\phi(X) = p(1|X, 1) = \sigma(g(X) - \zeta^p)$, and let $\psi(X) = q(1|X, 1) = \sigma(g(X) - \zeta)$.

Next, set $U = g(X)$ and denote by $\mu = p_{X|A=1} \circ g^{-1}$ the pushforward measure of $p_{X|A=1}$ by g . Introduce the deterministic functions $f(u) = \sigma(u - \zeta^p)$ and $h(u) = \sigma(u - \zeta)$ for $u \in \mathbb{R}$. Now, since

the standard logistic (sigmoid) function σ is monotonically increasing in its argument, both f and h are hence nondecreasing real-valued functions. So, Chebyshev's Association Inequality applies and gives that $\text{Cov}_\mu(f(U), h(U)) \geq 0$.

Finally, because $\phi(X) = f(U)$ and $\psi(X) = h(U)$, we consequently have that

$$\text{Cov}_{p_{X|A=1}}(\phi(X), \psi(X)) = \text{Cov}_\mu(f(U), h(U)) \geq 0,$$

which proves the claim. \square

Note that the lemma above is where the inequality in Theorem 4.3 arises. It holds with equality when $g(X)$ is almost surely constant.

Lemma B.3. *Suppose $Z \in (0, 1)$ is a random variable. Then,*

$$\mathbb{E}[\log(1 - Z)] = \log(1 - \mathbb{E}[Z]) - \frac{\text{Var}(Z)}{2(1 - \mathbb{E}[Z])^2} + \mathcal{O}(\mathbb{E}[(Z - \mathbb{E}[Z])^3])$$

and

$$\mathbb{E}[\log(Z)] = \log(\mathbb{E}[Z]) - \frac{\text{Var}(Z)}{2\mathbb{E}[Z]^2} + \mathcal{O}(\mathbb{E}[(Z - \mathbb{E}[Z])^3])$$

Proof. Since the function $\log(1 - z)$, $z \in (0, 1)$ is (at least) three times differentiable, we can compute a second order Taylor expansion about a value $\mu \in (0, 1)$:

$$\begin{aligned} \log(1 - z) &= \log(1 - \mu) - \frac{z - \mu}{1 - \mu} - \frac{(z - \mu)^2}{2(1 - \mu)^2} - \frac{1}{6} \cdot \frac{2}{(1 - \xi)^3} (z - \mu)^3 \\ &= \log(1 - \mu) - \frac{z - \mu}{1 - \mu} - \frac{(z - \mu)^2}{2(1 - \mu)^2} - \frac{(z - \mu)^3}{3(1 - \xi)^3} \end{aligned}$$

for some ξ between μ and z . Then, plugging in the random variable Z for z and $\mathbb{E}[Z]$ for μ , and taking an expectation, we have

$$\begin{aligned} \mathbb{E}[\log(1 - Z)] &= \log(1 - \mathbb{E}[Z]) - \frac{\mathbb{E}[(Z - \mathbb{E}[Z])^2]}{2(1 - \mathbb{E}[Z])^2} - \frac{\mathbb{E}[(Z - \mathbb{E}[Z])^3]}{3(1 - \xi_1)^3} \\ &= \log(1 - \mathbb{E}[Z]) - \frac{\text{Var}[Z]}{2(1 - \mathbb{E}[Z])^2} + \mathcal{O}(\mathbb{E}[(Z - \mathbb{E}[Z])^3]) \end{aligned}$$

where the linear term disappears from the first equality because its expectation is zero. Additionally, all expectations are well-defined because bounded random variables have finite moments of all orders.

The expansion for $\mathbb{E}[\log(Z)]$ is done similarly. \square

Lemma B.4. *Let $Z \in [0, 1]$, $\mu = \mathbb{E}[Z]$, $\mu_0 \in \mathbb{R}$, and $\Gamma \in \mathbb{R}$ subject to $\mu = \mu_0 - \Gamma$. Then,*

$$\text{Var}[Z] \leq (\mu_0 - \Gamma)(1 - \mu_0 + \Gamma).$$

Proof. Since $Z \in [0, 1]$, $Z^2 \leq Z$, $\mathbb{E}[Z^2] \leq \mathbb{E}[Z]$. This implies that

$$\text{Var}[Z] = \mathbb{E}[Z^2] - \mathbb{E}[Z]^2 \leq \mathbb{E}[Z](1 - \mathbb{E}[Z]) = \mu(1 - \mu).$$

Plugging in $\mu = \mu_0 - \Gamma$ gives the result. \square

C Proof of Lemma 4.1

Recall that we denote the binary cross-entropy (BCE) loss ℓ of a classifier f with respect to a sample (x, a, y) by

$$\ell(f, (x, a, y)) = -(y \log(f(x, a)) + (1 - y) \log(1 - f(x, a))).$$

Note that f can be a soft classifier that returns values in $[0, 1]$. Further recall that we denote the expected BCE of f with respect to a distribution $p_{X,A,Y}$ by

$$\mathcal{L}(p_{X,A,Y}, f) = -\mathbb{E}_{x,a,y \sim p_{X,A,Y}} [y \log(f(x, a)) + (1 - y) \log(1 - f(x, a))],$$

and this notation $\mathcal{L}(\cdot, \cdot)$ is used analogously for other distributions and classifiers.

Proof. We split the proof into four steps.

Step 1: Decomposition. We can decompose the BCE loss of a classifier $\hat{f} \in \mathcal{F}$ on a distribution $p_{X,A,Y}$ as follows

$$H(p_{X,A,Y}, \hat{f}) = \underbrace{(H(p_{X,A,Y}, \hat{f}) - H(q_{XAY}, \hat{f}))}_{\text{loss of } \hat{f} \text{ due to distribution shift}} \quad (5)$$

$$+ \underbrace{(H(q_{XAY}, \hat{f}) - H(q_{XAY}, q_{1|X,A}))}_{\text{train loss of } \hat{f} \text{ relative to Bayes optimal}} \quad (6)$$

$$+ \underbrace{(H(q_{XAY}, q_{1|X,A}) - H(p_{X,A,Y}, q_{1|X,A}))}_{\text{loss of Bayes optimal } q_{1|X,A} \text{ due to distribution shift}} \quad (7)$$

$$+ \underbrace{(H(p_{X,A,Y}, q_{1|X,A}) - H(p_{X,A,Y}, p_{1|X,A}))}_{\text{difference in test loss of Bayes optimal classifiers}} \quad (8)$$

$$+ \underbrace{H(p_{X,A,Y}, p_{1|X,A})}_{\text{irreducible test loss}}, \quad (9)$$

by simply adding and subtracting terms, where we slightly abuse notation to let $q_{1|X,A}$ denote a (soft) classifier where the prediction for (x, a) is given by $q_{Y|X,A}(1|x, a)$.

As written below each term, (5) can be viewed as the loss of \hat{f} due to distribution shift between the train distribution $q_{X,A,Y}$ and test distribution $p_{X,A,Y}$; (6) is the difference in loss between \hat{f} on the train distribution and the Bayes optimal classifier (also relative to the train distribution), which can be viewed as the loss due to the choice of model family \mathcal{F} ; (7) also captures loss due to distribution shift, but for the Bayes optimal classifier of $q_{1|X,A}$; (8) gives difference in test loss between the Bayes optimal classifier that is optimal with respect to the train distribution and one that is optimal with respect to the test distribution, which can be viewed in some sense as the irreducible generalization loss; and (9) gives the irreducible test loss of the Bayes optimal classifier $p_{1|X,A}$ (that is optimal with respect the test distribution).

Step 2: Expanding (5) and (7). Focusing on just two of the terms above, we have

$$\begin{aligned} (5) + (7) &= -\mathbb{E}_{x,a,y \sim p_{X,A,Y}} [y \log \hat{f}(x, a) + (1-y) \log(1 - \hat{f}(x, a))] \\ &\quad + \mathbb{E}_{x,a,y \sim q_{X,A,Y}} [y \log \hat{f}(x, a) + (1-y) \log(1 - \hat{f}(x, a))] \\ &\quad - \mathbb{E}_{x,a,y \sim q_{X,A,Y}} [y \log q_{Y|X,A}(1|x, a) + (1-y) \log(1 - q_{Y|X,A}(1|x, a))] \\ &\quad + \mathbb{E}_{x,a,y \sim p_{X,A,Y}} [y \log q_{Y|X,A}(1|x, a) + (1-y) \log(1 - q_{Y|X,A}(1|x, a))] \\ &= - \int_{x,a,y} (p_{X,A,Y}(x, a, y) - q_{X,A,Y}(x, a, y)) \\ &\quad \left(y \log \hat{f}(x, a) + (1-y) \log(1 - \hat{f}(x, a)) \right) dx da dy \\ &\quad + \int_{x,a,y} (p_{X,A,Y}(x, a, y) - q_{X,A,Y}(x, a, y)) \\ &\quad \left(y \log q_{Y|X,A}(1|x, a) + (1-y) \log(1 - q_{Y|X,A}(1|x, a)) \right) dx da dy \\ &= \int_{x,a,y} (p_{X,A,Y}(x, a, y) - q_{X,A,Y}(x, a, y)) \\ &\quad \left(y \log \left(\frac{q_{Y|X,A}(1|x, a)}{\hat{f}(x, a)} \right) + (1-y) \log \left(\frac{1 - q_{Y|X,A}(1|x, a)}{1 - \hat{f}(x, a)} \right) \right) dx da dy \\ &= \int_{x,a,y} q_{X,A,Y}(x, a, y) (w(x, a, y) - 1) \\ &\quad \left(y \log \left(\frac{q_{Y|X,A}(1|x, a)}{\hat{f}(x, a)} \right) + (1-y) \log \left(\frac{1 - q_{Y|X,A}(1|x, a)}{1 - \hat{f}(x, a)} \right) \right) dx da dy \end{aligned}$$

$$\begin{aligned}
&= \mathbb{E}_{q_{X,A,Y}} \left[(w(x, a, y) - 1) \left(y \log \left(\frac{q_{Y|X,A}(1|x, a)}{\hat{f}(x, a)} \right) \right. \right. \\
&\quad \left. \left. + (1-y) \log \left(\frac{1 - q_{Y|X,A}(1|x, a)}{1 - \hat{f}(x, a)} \right) \right) \right],
\end{aligned}$$

where $w(x, a, y) = p_{X,A,Y}(x, a, y) / q_{X,A,Y}(x, a, y)$. Let

$$R := w(x, a, y) - 1 \quad \text{and} \quad S := y \log \left(\frac{q_{Y|X,A}(1|x, a)}{\hat{f}(x, a)} \right) + (1-y) \log \left(\frac{1 - q_{Y|X,A}(1|x, a)}{1 - \hat{f}(x, a)} \right).$$

Then, by invoking Theorem B.1—which applies because S is absolutely integrable under the condition given in the lemma statement and because $p_{X,A,Y} \ll q_{X,A,Y}$ —we have that

$$\mathbb{E}_{q_{X,A,Y}}[RS] = \mathbb{E}_{q_{X,A,Y}}[R]\mathbb{E}_{q_{X,A,Y}}[S] \iff \mathbb{E}_{q_{X,A,Y}}[S] = \mathbb{E}_{p_{X,A,Y}}[S].$$

By the condition given in the lemma statement, $\mathbb{E}_{q_{X,A,Y}}[S] = \mathbb{E}_{p_{X,A,Y}}[S]$ and hence we obtain

$$(5) + (7) = \mathbb{E}_{q_{X,A,Y}}[RS] = \mathbb{E}_{q_{X,A,Y}}[R]\mathbb{E}_{q_{X,A,Y}}[S] = 0.$$

where the last equality is because $\mathbb{E}_{q_{X,A,Y}}[R] = 0$, as shown in the proof of Theorem B.1.

Step 3: Expanding (8). The term (8) can be written as

$$- \int_{x,a,y} p_{X,A,Y}(x, a, y) \left[y \log \frac{q_{Y|X,A}(1|x, a)}{p_{Y|X,A}(1|x, a)} + (1-y) \log \frac{q_{Y|X,A}(0|x, a)}{p_{Y|X,A}(0|x, a)} \right] dx da dy.$$

Substituting for possible values of $y \in \{0, 1\}$ gives

$$\begin{aligned}
&- \int_{x,a} p_{X,A}(x, a) p_{Y|X,A}(0|x, a) \left[\log \frac{q_{Y|X,A}(0|x, a)}{p_{Y|X,A}(0|x, a)} \right] dx da \\
&\quad - \int_{x,a} p_{X,A}(x, a) p_{Y|X,A}(1|x, a) \left[\log \frac{q_{Y|X,A}(1|x, a)}{p_{Y|X,A}(1|x, a)} \right] dx da \\
&= - \int_{x,a} p_{X,A}(x, a) (1 - p_{Y|X,A}(1|x, a)) \left[\log \frac{q_{Y|X,A}(0|x, a)}{p_{Y|X,A}(0|x, a)} \right] dx da \\
&\quad - \int_{x,a} p_{X,A}(x, a) p_{Y|X,A}(1|x, a) \left[\log \frac{q_{Y|X,A}(1|x, a)}{p_{Y|X,A}(1|x, a)} \right] dx da \\
&= - \int_{x,a} p_{X,A}(x, a) \left[(1 - p_{Y|X,A}(1|x, a)) \left[\log \frac{1 - q_{Y|X,A}(1|x, a)}{1 - p_{Y|X,A}(1|x, a)} \right] \right. \\
&\quad \left. + p_{Y|X,A}(1|x, a) \left[\log \frac{q_{Y|X,A}(1|x, a)}{p_{Y|X,A}(1|x, a)} \right] \right] \\
&= \mathbb{E}_{x,a \sim p_{X,A}} [\text{KL}(p_{Y|X,A}(1|x, a) \parallel q_{Y|X,A}(1|x, a))],
\end{aligned}$$

where we use $\text{KL}(r \parallel s)$ to denote the KL divergence between the Bernoulli(r) and Bernoulli(s) distributions.

Step 4: Putting it together. Combining Steps 1-3,

$$\begin{aligned}
&H(p_{X,A,Y}, \hat{f}) \\
&= (5) + (6) + (7) + (8) + (9) \\
&= (6) + (8) + (9) \\
&= H(q_{XAY}, \hat{f}) - H(q_{XAY}, q_{1|X,A}) \\
&\quad + \mathbb{E}_{x,a \sim p_{X,A}} [\text{KL}(p_{Y|x,a} \parallel q_{Y|x,a})] + H(p_{X,A,Y}, p_{1|X,A}),
\end{aligned}$$

which concludes the proof. \square

D Proof of Theorem 4.3

Proof. In this proof, we use Theorem 4.1 to express the BCE loss in terms of the train distribution parameter ζ , then likewise express the demographic parity gap in terms of ζ . Combining these representations allows us to express the BCE loss directly in terms of the demographic parity gap. We note that, by definition of our data-generating process, $p_{X,A,Y} \ll q_{X,A,Y}^\zeta$ for all ζ .

Step 1: Simplifying BCE loss. Recall from Theorem 4.1 that

$$\begin{aligned} H(p_{X,A,Y}, \hat{f}^\zeta) &= (H(q_{XAY}^\zeta, \hat{f}^\zeta) - H(q_{XAY}^\zeta, q_{1|X,A}^\zeta)) \\ &\quad + \mathbb{E}_{x,a \sim p_{X,A}} \left[\text{KL} \left(p_{Y|x,a} \middle\| q_{Y|x,a}^\zeta \right) \right] + H(p_{X,A,Y}, p_{1|X,A}). \end{aligned}$$

We begin by characterizing each component of this expression.

First, by Theorem 4.2, $H(q_{XAY}^\zeta, \hat{f}^\zeta) - H(q_{XAY}^\zeta, q_{1|X,A}^\zeta)$ can be written as a constant $c_1(\mathcal{F}, D)$ that depends only on the model class \mathcal{F} and the amount of training data D .

Second, we note that $H(p_{X,A,Y}, p_{1|X,A})$ can also be treated as a constant $c_2(p)$ that depends only on the test distribution p and not on the model class \mathcal{F} or the train distribution q^ζ . This gives

$$H(p_{X,A,Y}, \hat{f}^\zeta) = c_1(\mathcal{F}, D) + \mathbb{E}_{x,a \sim p_{X,A}} \left[\text{KL} \left(p_{Y|x,a} \middle\| q_{Y|x,a}^\zeta \right) \right] + c_2(p), \quad (10)$$

where

$$\begin{aligned} c_1(\mathcal{F}, D) &:= H(q_{XAY}^\zeta, \hat{f}^\zeta) - H(q_{XAY}^\zeta, q_{1|X,A}^\zeta), \\ c_2(p) &:= H(p_{X,A,Y}, p_{1|X,A}). \end{aligned}$$

Thus, it remains only to characterize the expected KL divergence term and write it in terms of the demographic parity gap. That will be the goal of the following steps.

Step 2: Rewriting the KL divergence term.

$$\begin{aligned} &\mathbb{E}_{x,a \sim p_{X,A}} \left[\text{KL} \left(p_{Y|x,a} \middle\| q_{Y|x,a}^\zeta \right) \right] \\ &= - \int_{x,a} p_{X,A}(x,a) \left[(1 - p_{Y|X,A}(1|x,a)) \log \frac{1 - q_{Y|X,A}^\zeta(1|x,a)}{1 - p_{Y|X,A}(1|x,a)} \right. \\ &\quad \left. + p_{Y|X,A}(1|x,a) \log \frac{q_{Y|X,A}^\zeta(1|x,a)}{p_{Y|X,A}(1|x,a)} \right] \\ &= -\mathbb{E}_{x,a \sim p_{X,A}} [(1 - p_{Y|X,A}(1|x,a)) \log (1 - q_{Y|X,A}^\zeta(1|x,a)) \\ &\quad + p_{Y|X,A}(1|x,a) \log q_{Y|X,A}^\zeta(1|x,a)] + c_3(p), \quad (11) \end{aligned}$$

where

$$\begin{aligned} c_3(p) &:= \int_{x,a} p_{X,A}(x,a) \left[(1 - p_{Y|X,A}(1|x,a)) \log (1 - p_{Y|X,A}(1|x,a)) \right. \\ &\quad \left. + p_{Y|X,A}(1|x,a) \log (p_{Y|X,A}(1|x,a)) \right], \end{aligned}$$

is a constant that depends only on the test distribution p . Recalling from our data generating process given in Section 4 that $p(A=1) = \pi$, (11) becomes

$$\begin{aligned} &\mathbb{E}_{x,a \sim p_{X,A}} \left[\text{KL} \left(p_{Y|x,a} \middle\| q_{Y|x,a}^\zeta \right) \right] \\ &= -\mathbb{E}_{x,a \sim p_{X,A}} [(1 - p_{Y|X,A}(1|x,a)) \log (1 - q_{Y|X,A}^\zeta(1|x,a)) \\ &\quad + p_{Y|X,A}(1|x,a) \log q_{Y|X,A}^\zeta(1|x,a)] + c_3(p) \\ &= \pi \left(-\mathbb{E}_{x \sim p_{X|A}} [(1 - p_{Y|X,A}(1|x,A)) \log (1 - q_{Y|X,A}^\zeta(1|x,A)) \right. \\ &\quad \left. + p_{Y|X,A}(1|x,A) \log q_{Y|X,A}^\zeta(1|x,A)] \right) + c_3(p) \end{aligned}$$

$$+ p_{Y|X,A}(1|x, A) \log q_{Y|X,A}^\zeta(1|x, A) \mid A = 1 \Big] \Big) + c_4(p), \quad (12)$$

where the last line follows from the fact that, when $A = 0$, the q distribution no longer depends on ζ (cf. our data generating process for Y given in Section 4) such that

$$\begin{aligned} c_4(p) := c_3(p) + (1 - \pi) & \left(-\mathbb{E}_{x \sim p_{X|A}} \left[(1 - p_{Y|X,A}(1|x, A)) \log(1 - q_{Y|X,A}^\zeta(1|x, A)) \right. \right. \\ & \left. \left. + p_{Y|X,A}(1|x, A) \log q_{Y|X,A}^\zeta(1|x, A) \mid A = 0 \right] \right). \end{aligned}$$

Step 3: Upper bounding KL divergence term. By the definition of covariance,

$$\begin{aligned} \mathbb{E}_{x \sim p_{X|A}} \left[(1 - p_{Y|X,A}(1|x, A)) \log(1 - q_{Y|X,A}^\zeta(1|x, A)) \mid A = 1 \right] \\ = \mathbb{E}_{x \sim p_{X|A}} \left[(1 - p_{Y|X,A}(1|x, A)) \mid A = 1 \right] \mathbb{E}_{x \sim p_{X|A}} \left[\log(1 - q_{Y|X,A}^\zeta(1|x, A)) \mid A = 1 \right] \\ + \text{Cov}_{x \sim p_{X|A}} \left((1 - p_{Y|X,A}(1|x, A)), \log(1 - q_{Y|X,A}^\zeta(1|x, A)) \mid A = 1 \right). \end{aligned}$$

By Lemma B.2, and our data-generating process as given in the theorem statement and Section 4, the covariance term is non-negative. Therefore,

$$\begin{aligned} \mathbb{E}_{x \sim p_{X|A}} \left[(1 - p_{Y|X,A}(1|x, A)) \log(1 - q_{Y|X,A}^\zeta(1|x, A)) \mid A = 1 \right] \\ \geq \mathbb{E}_{x \sim p_{X|A}} \left[(1 - p_{Y|X,A}(1|x, A)) \mid A = 1 \right] \mathbb{E}_{x \sim p_{X|A}} \left[\log(1 - q_{Y|X,A}^\zeta(1|x, A)) \mid A = 1 \right]. \end{aligned} \quad (13)$$

One can apply analogous reasoning to show, again, by Theorem B.2 that

$$\begin{aligned} \mathbb{E}_{x \sim p_{X|A}} \left[p_{Y|X,A}(1|x, A) \log q_{Y|X,A}^\zeta(1|x, A) \mid A = 1 \right] \\ \geq \mathbb{E}_{x \sim p_{X|A}} \left[p_{Y|X,A}(1|x, A) \mid A = 1 \right] \mathbb{E}_{x \sim p_{X|A}} \left[\log q_{Y|X,A}^\zeta(1|x, A) \mid A = 1 \right]. \end{aligned}$$

(Note that the two applications of Theorem B.2 above are where the inequality in Theorem 4.3 arises. Therefore, if one wishes to remove the inequality or provide a high-probability version of our result that holds with equality, one should address Theorem B.2.) Therefore, from (12),

$$\begin{aligned} \mathbb{E}_{x,a \sim p_{X,A}} \left[\text{KL} \left(p_{Y|x,a} \mid\mid q_{Y|x,a}^\zeta \right) \right] \\ \leq -\pi \left(\mathbb{E}_{x \sim p_{X|A}} \left[(1 - p_{Y|X,A}(1|x, A)) \mid A = 1 \right] \mathbb{E}_{x \sim p_{X|A}} \left[\log(1 - q_{Y|X,A}^\zeta(1|x, A)) \mid A = 1 \right] \right. \\ \left. + \mathbb{E}_{x \sim p_{X|A}} \left[p_{Y|X,A}(1|x, A) \mid A = 1 \right] \mathbb{E}_{x \sim p_{X|A}} \left[\log q_{Y|X,A}^\zeta(1|x, A) \mid A = 1 \right] \right) + c_4(p) \\ = -\pi(1 - c_5(p)) \mathbb{E}_{x \sim p_{X|A}} \left[\log(1 - q_{Y|X,A}^\zeta(1|x, A)) \mid A = 1 \right] \\ - \pi c_5(p) \mathbb{E}_{x \sim p_{X|A}} \left[\log q_{Y|X,A}^\zeta(1|x, A) \mid A = 1 \right] + c_4(p), \end{aligned}$$

where $c_5(p) := \mathbb{E}_{x \sim p_{X|A}} [p_{Y|X,A}(1|x, A) \mid A = 1]$.

Step 4: Moving the expectation inside the log. Then, we apply Theorem B.3, using $q_{Y|X,A}^\zeta(1 \mid x, 1)$ as the Z in the statement of the lemma, and noting that it is a random variable that takes values between 0 and 1, as required by the lemma. For ease of notation, let

$$\begin{aligned} \bar{q}_1 &:= \mathbb{E}_{x \sim p_{X|A}} \left[q_{Y|X,A}^\zeta(1|x, A) \mid A = 1 \right], \\ \bar{q}_0 &:= \mathbb{E}_{x \sim p_{X|A}} \left[q_{Y|X,A}^\zeta(1|x, A) \mid A = 0 \right], \\ V &:= \text{Var}_{x \sim p_{X|A}} \left[q_{Y|X,A}^\zeta(1|x, A) \mid A = 1 \right]. \end{aligned} \quad (14)$$

Then, Theorem B.3 gives

$$\mathbb{E}_{x,a \sim p_{X,A}} \left[\text{KL} \left(p_{Y|x,a} \mid\mid q_{Y|x,a}^\zeta \right) \right]$$

$$\begin{aligned}
&\leq -\pi(1 - c_5(p)) \left(\log(1 - \bar{q}_1) - \frac{V}{2(1 - \bar{q}_1)^2} \right) - \pi c_5(p) \left(\log(\bar{q}_1) - \frac{V}{2\bar{q}_1^2} \right) \\
&\quad + \mathcal{O} \left(\mathbb{E}_{x \sim p_{X|A}} \left[(q_{Y|X,A}^\zeta(1|x, A) - \bar{q}_1)^3 \mid A = 1 \right] \right) + c_4(p). \tag{15}
\end{aligned}$$

Now that the KL divergence term is upper bounded, we proceed to characterize the demographic parity gap, and then substitute it into the KL divergence term.

Step 5: Characterizing demographic parity gap. The definition of demographic parity gap is

$$\Delta(p_{X,A,Y}, \hat{f}^\zeta) := \left| \mathbb{E}_{x \sim p_{X|A}} [\hat{f}^\zeta(x, A) \mid A = 1] - \mathbb{E}_{x \sim p_{X|A}} [\hat{f}^\zeta(x, A) \mid A = 0] \right|.$$

We can rewrite it as

$$\begin{aligned}
&\mathbb{E}_{x \sim p_{X|A}} [\hat{f}^\zeta(x, A) \mid A = 1] - \mathbb{E}_{x \sim p_{X|A}} [\hat{f}^\zeta(x, A) \mid A = 0] \\
&= \mathbb{E}_{x \sim p_{X|A}} [q_{Y|X,A}^\zeta(1|x, A) \mid A = 1] - \mathbb{E}_{x \sim p_{X|A}} [q_{Y|X,A}^\zeta(1|x, A) \mid A = 0] \\
&\quad + (\mathbb{E}_{x \sim p_{X|A}} [\hat{f}^\zeta(x, A) \mid A = 1] - \mathbb{E}_{x \sim p_{X|A}} [q_{Y|X,A}^\zeta(1|x, A) \mid A = 1]) \tag{16} \\
&\quad + (\mathbb{E}_{x \sim p_{X|A}} [q_{Y|X,A}^\zeta(1|x, A) \mid A = 0] - \mathbb{E}_{x \sim p_{X|A}} [\hat{f}^\zeta(x, A) \mid A = 0]). \tag{17}
\end{aligned}$$

By Theorem 4.2,

$$\begin{aligned}
&\mathbb{E}_{x \sim p_{X|A}} [\hat{f}^\zeta(x, A) \mid A = 1] - \mathbb{E}_{x \sim p_{X|A}} [\hat{f}^\zeta(x, A) \mid A = 0] \\
&= \mathbb{E}_{x \sim p_{X|A}} [q_{Y|X,A}^\zeta(1|x, A) \mid A = 1] - \mathbb{E}_{x \sim p_{X|A}} [q_{Y|X,A}^\zeta(1|x, A) \mid A = 0].
\end{aligned}$$

By our data generating process given in Theorem 4.3, in which A mediates the effect of ζ and larger values of ζ result in lower positive classification rates,

$$\mathbb{E}_{x \sim p_{X|A}} [q_{Y|X,A}^\zeta(1|x, A) \mid A = 0] \geq \mathbb{E}_{x \sim p_{X|A}} [q_{Y|X,A}^\zeta(1|x, A) \mid A = 1].$$

for $\zeta \geq 0$. Therefore,

$$\Delta(p_{X,A,Y}, \hat{f}^\zeta) = \bar{q}_0 - \bar{q}_1. \tag{18}$$

Note that if we relaxed the second condition in Theorem 4.2 to allow for an additive constant, this would allow us to complete our analysis but with more bookkeeping, as the expression above would have two cases to ensure $\Delta \geq 0$.

Step 6: Combining and rewriting BCE loss in terms of $\Delta(p_{X,A,Y}, \hat{f}^\zeta)$. We can now substitute this expression for $\Delta(p_{X,A,Y}, \hat{f}^\zeta)$ from (18) into the BCE loss. From (15), we have

$$\begin{aligned}
&\mathbb{E}_{x,a \sim p_{X,A}} \left[\text{KL} \left(p_{Y|x,a} \mid\mid q_{Y|x,a}^\zeta \right) \right] \\
&\leq -\pi(1 - c_5(p)) \log(1 - \bar{q}_0 + \Delta(p_{X,A,Y}, \hat{f}^\zeta)) + \frac{\pi(1 - c_5(p))V}{2(1 - \bar{q}_0 + \Delta(p_{X,A,Y}, \hat{f}^\zeta))^2} \\
&\quad - \pi c_5(p) \log(\bar{q}_0 - \Delta(p_{X,A,Y}, \hat{f}^\zeta)) + \frac{\pi c_5(p)V}{2(\bar{q}_0 - \Delta(p_{X,A,Y}, \hat{f}^\zeta))^2} \\
&\quad + c_4(p) + \mathcal{O} \left(\mathbb{E}_{x \sim p_{X|A}} \left[(q_{Y|X,A}^\zeta(1|x, A) - \bar{q}_1)^3 \mid A = 1 \right] \right).
\end{aligned}$$

We use Theorem B.4 with $Z = q_{Y|X,A}^\zeta(1|x, A)$, $\mu = \bar{q}_1$, $\mu_0 = \bar{q}_0$, $\Gamma = \Delta = \bar{q}_0 - \bar{q}_1$ by (18), and that the expectations in Theorem B.4 are taken with respect to $p_{X|A=1}$ to get

$$V \leq (c_6(p) - \Delta)(1 - c_6(p) + \Delta(p_{X,A,Y}, \hat{f}^\zeta)),$$

where $c_6(p) = \bar{q}_0$. Therefore,

$$\begin{aligned}
&\mathbb{E}_{x,a \sim p_{X,A}} \left[\text{KL} \left(p_{Y|x,a} \mid\mid q_{Y|x,a}^\zeta \right) \right] \\
&\leq -\pi(1 - c_5(p)) \log(1 - c_6(p) + \Delta(p_{X,A,Y}, \hat{f}^\zeta))
\end{aligned}$$

$$\begin{aligned}
& + \frac{\pi(1 - c_5(p))(c_6(p) - \Delta(p_{X,A,Y}, \hat{f}^\zeta))(1 - c_6(p) + \Delta(p_{X,A,Y}, \hat{f}^\zeta))}{2(1 - c_6(p) + \Delta(p_{X,A,Y}, \hat{f}^\zeta))^2} \\
& - \pi c_5(p) \log(c_6(p) - \Delta(p_{X,A,Y}, \hat{f}^\zeta)) \\
& + \frac{\pi c_5(p)(c_6(p) - \Delta(p_{X,A,Y}, \hat{f}^\zeta))(1 - c_6(p) + \Delta(p_{X,A,Y}, \hat{f}^\zeta))}{2(c_6(p) - \Delta(p_{X,A,Y}, \hat{f}^\zeta))^2} \\
& + c_4(p) + \mathcal{O}\left(\mathbb{E}_{x \sim p_{X|A}} \left[(q_{Y|X,A}^\zeta(1|x, A) - \bar{q}_1)^3 \mid A = 1 \right]\right), \tag{19}
\end{aligned}$$

where we recall all constants:

$$\begin{aligned}
c_2(p) &= H(p_{X,A,Y}, p_{1|X,A}), \\
c_3(p) &= \mathbb{E}_{x,a \sim p_{X,A}} \left[(1 - p_{Y|X,A}(1|x, a)) \log(1 - p_{Y|X,A}(1|x, a)) \right. \\
&\quad \left. + p_{Y|X,A}(1|x, a) \log(p_{Y|X,A}(1|x, a)) \right], \\
c_4(p) &= c_3(p) - (1 - \pi) \mathbb{E}_{x \sim p_{X|A}} \left[(1 - p_{Y|X,A}(1|x, A)) \log(1 - q_{Y|X,A}^\zeta(1|x, A)) \right. \\
&\quad \left. + p_{Y|X,A}(1|x, A) \log q_{Y|X,A}^\zeta(1|x, A) \mid A = 0 \right], \\
c_5(p) &= \mathbb{E}_{x \sim p_{X|A}} [p_{Y|X,A}(1|x, A) \mid A = 1] \\
c_6(p) &= \mathbb{E}_{x \sim p_{X|A}} \left[q_{Y|X,A}^\zeta(1|x, A) \mid A = 0 \right]
\end{aligned}$$

Putting it all together, combining (10) and (19),

$$\begin{aligned}
H(p_{X,A,Y}, \hat{f}^\zeta) &\leq B(\mathcal{F}, D) - c \cdot c' \log(1 - c'' + \underline{\Delta}) - c \cdot (1 - c') \log(c'' - \underline{\Delta}) \\
&\quad + (c'' - \underline{\Delta})(1 - c'' + \underline{\Delta}) \left(\frac{c \cdot c'}{2(1 - c'' + \underline{\Delta})^2} + \frac{c \cdot (1 - c')}{2(c'' - \underline{\Delta})^2} \right) \\
&\quad + \mathcal{O}\left(\mathbb{E}_{x \sim p_{X|A}} \left[(q_{Y|X,A}^\zeta(1|x, A) - \bar{q}_1)^3 \mid A = 1 \right]\right),
\end{aligned}$$

where

$$\begin{aligned}
B(\mathcal{F}, D) &:= c_1(\mathcal{F}, D) + c_2(p) + c_4(p) \\
&= c_1(\mathcal{F}, D) + H(p_{X,A,Y}, p_{1|X,A}) \\
&\quad - (1 - \pi) \mathbb{E}_{x \sim p_{X|A}} \left[(1 - p_{Y|X,A}(1|x, A)) \log(1 - q_{Y|X,A}^\zeta(1|x, A)) \right. \\
&\quad \left. + p_{Y|X,A}(1|x, A) \log q_{Y|X,A}^\zeta(1|x, A) \mid A = 0 \right] \\
&\quad + \mathbb{E}_{x,a \sim p_{X,A}} \left[(1 - p_{Y|X,A}(1|x, a)) \log(1 - p_{Y|X,A}(1|x, a)) \right. \\
&\quad \left. + p_{Y|X,A}(1|x, a) \log(p_{Y|X,A}(1|x, a)) \right] \\
c &:= \pi \\
c' &:= 1 - \mathbb{E}_{x \sim p_{X|A}} [p_{Y|X,A}(1|x, A) \mid A = 1] \in [0, 1] \\
c'' &:= \mathbb{E}_{x \sim p_{X|A}} [q_{Y|X,A}^\zeta(1|x, A) \mid A = 0] \in [0, 1]
\end{aligned}$$

$c, c', c'' \geq 0$. Note that the constants may not correspond exactly to the stated quantities above, e.g., due to the note below (18). \square

E Additional Experimental Details and Results

E.1 Simulations

In this section, we provide further simulations, using the same procedure as given in Section 6.1.

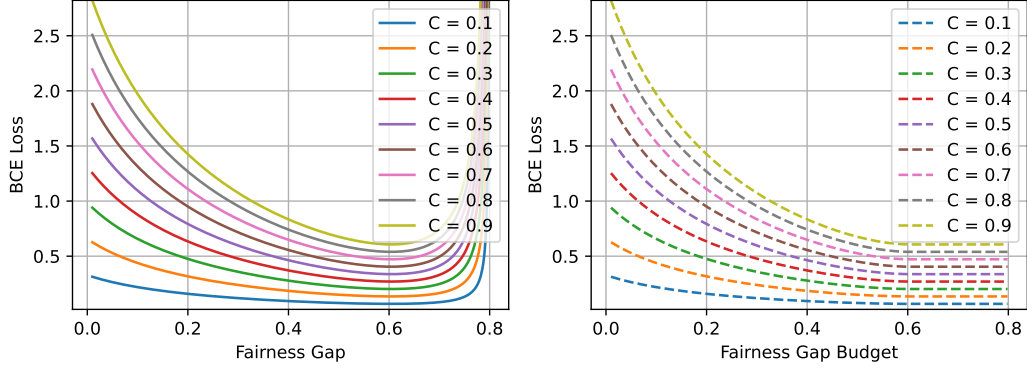


Figure 7: Simulations showing the shape of the closed-form expression for the Pareto frontier given in Theorem 4.3 for fixed values of $c'' = C_7 = 0.9$ and $c'' = 0.8$ while varying c . The left plot shows the precise closed-form, which is the lowest achievable loss among classifiers that have *exactly* the fairness gap value on the x-axis. The right plot shows lowest achievable loss among classifiers that satisfy the fairness gap *budget* on the x-axis.

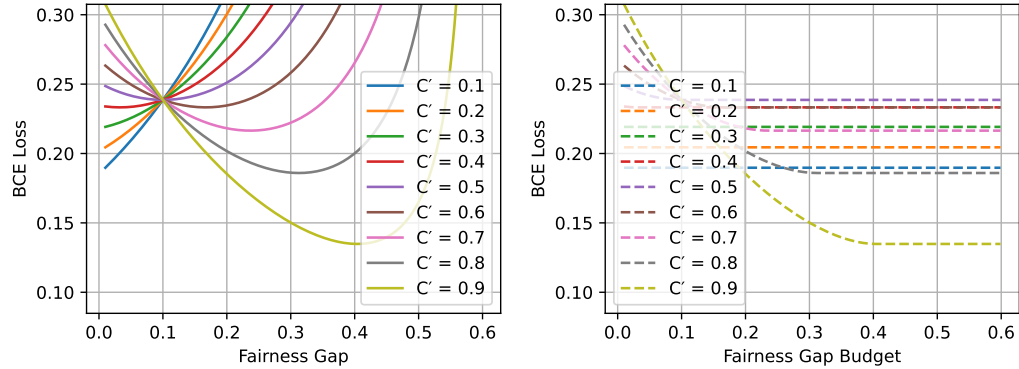


Figure 8: Simulations showing the shape of the closed-form expression for the Pareto frontier given in Theorem 4.3 for fixed values of $c = 0.2$ and $c'' = 0.6$ while varying C' . The left plot shows the precise closed-form, which is the lowest achievable loss among classifiers that have *exactly* the fairness gap value on the x-axis. The right plot shows lowest achievable loss among classifiers that satisfy the fairness gap *budget* on the x-axis.

E.2 Synthetic experiments

In this section, we provide additional details on the setup for the synthetic experiments in Figure 6 as well as additional results below.

E.3 Model Architecture and Training

We used Pytorch to train our models. To test the scaling law, we trained models under 4 different MLP configurations, each with two hidden layers and ReLU activations, with a sigmoid output for binary classification:

- [80, 80] hidden units (8080 total parameters)
- [160, 160] hidden units (28960 total parameters)
- [320, 320] hidden units (109120 total parameters)
- [640, 640] hidden units (423040 total parameters)

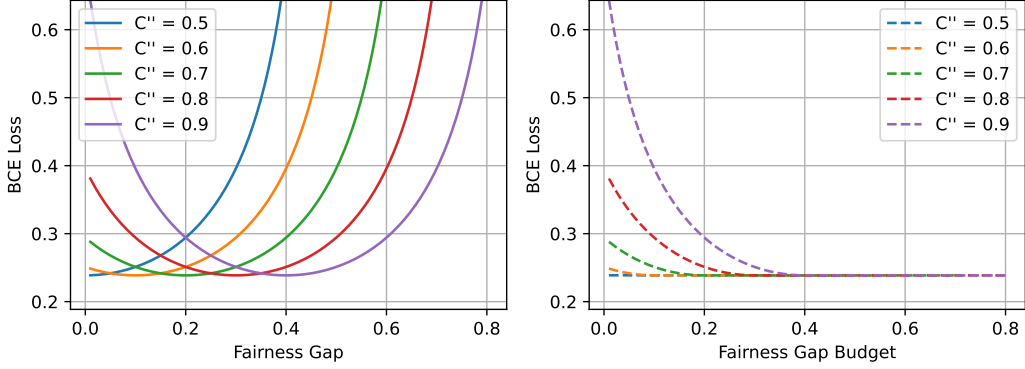


Figure 9: Simulations showing the shape of the closed-form expression for the Pareto frontier given in Theorem 4.3 for fixed values of $c = 0.2$ and $c'' = C_7 = 0.5$ while varying c'' . The left plot shows the precise closed-form, which is the lowest achievable loss among classifiers that have *exactly* the fairness gap value on the x-axis. The right plot shows lowest achievable loss among classifiers that satisfy the fairness gap *budget* on the x-axis.

For each architecture and λ value, the data is split into training (65%), validation (15%), and test (20%) sets. The models are trained for 30 epochs using the Adam optimizer with a learning rate of 0.001 and a batch size of 256, selecting the model with the lowest validation loss over the training epochs. We repeat each configuration over 3 random seeds and use all trials to find the Pareto frontier, resulting in 300 models per model size and 1200 models total.

E.3.1 Additional Results

We test on two combinations of ζ and π values.

We show results below. Interestingly, we found that the typical scaling law $N^{-0.5}$ did not necessarily fit our results perfectly, so we indicate the exponent used in each figure caption.

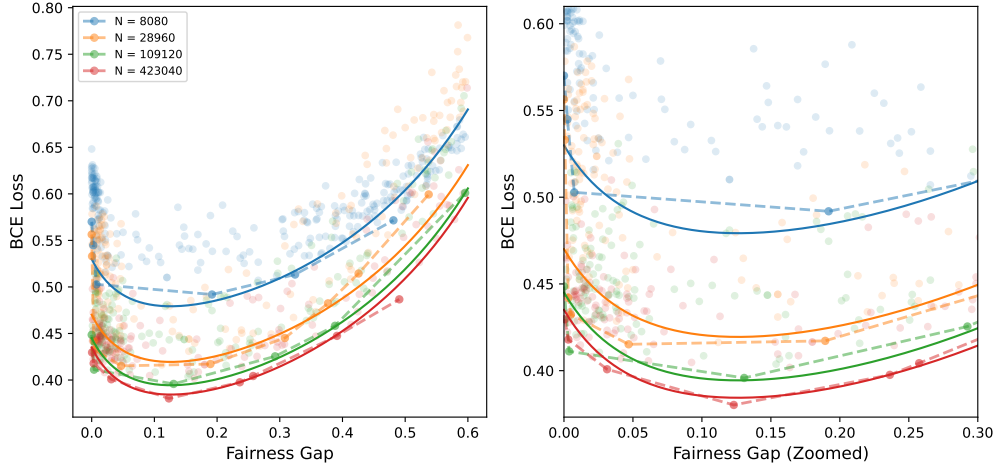


Figure 10: Pareto frontier for different model sizes under $(\pi = 0.2)$ and bias strength $\zeta = 0.5$. Each point corresponds to a trained model with a different fairness regularization weight λ . The dashed lines show the empirical Pareto frontier, created by finding the lower convex hull of all the points. The solid lines show fitted curves to the points on the Pareto frontier using Theorem 4.3 with $c = C_5 = 0.16$, $c' = C_6 = 0.11$, $c'' = C_7 = 0.92$, with bias $C_1 = -0.285$, $C_2 = 55$, $C_3 = 0.7$, and $C_4 = 0.5$. The left panel shows the frontier across the range of Δ , while the right panel zooms in on $\Delta \in [0, 0.3]$. The fitted curve mimics the empirical data well though it is imperfect. We found that there were many possible fits, depending on the precise choice. We show another possible fit in Figure 11 below.

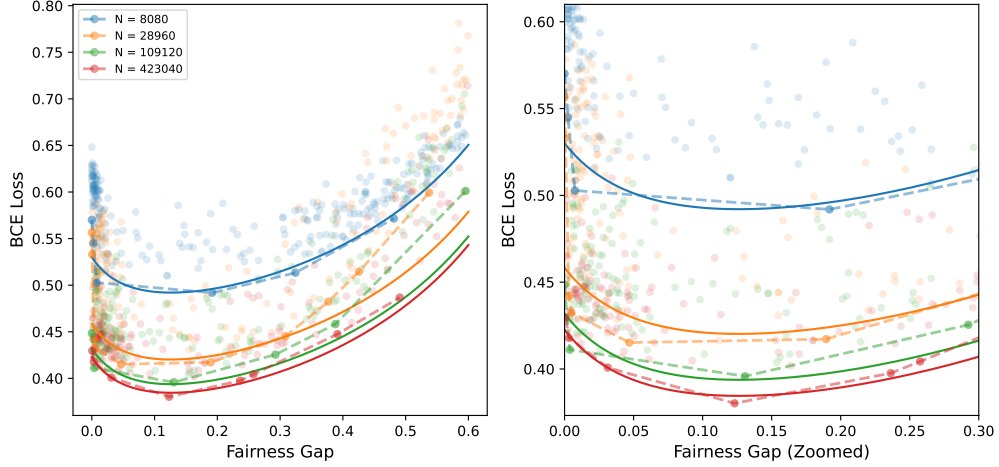


Figure 11: Pareto frontier for different model sizes under $(\pi = 0.2)$ and bias strength $\zeta = 0.5$. Each point corresponds to a trained model with a different fairness regularization weight λ . The dashed lines show the empirical Pareto frontier, created by finding the lower convex hull of all the points. The solid lines show fitted curves to the points on the Pareto frontier using Theorem 4.3 with $c = C_5 = 0.12$, $c' = C_6 = 0.11$, $c'' = C_7 = 0.92$, with bias $C_1 = -1.205$, $C_2 = 150$, $C_3 = 0.8$, and $C_4 = 0.5$. The left panel shows the frontier across the range of Δ , while the right panel zooms in on $\Delta \in [0, 0.3]$. The fitted curve is intentionally chosen to lower bound the larger models. That is, it fits to the small model curve, then uses it to extrapolate the larger model curve; we do so to exhibit one possible way to fit the curves since our training procedure was not optimized for the larger models and, as such, our empirical Pareto frontier is likely not optimal. We show another possible fit in Figure 6 below.

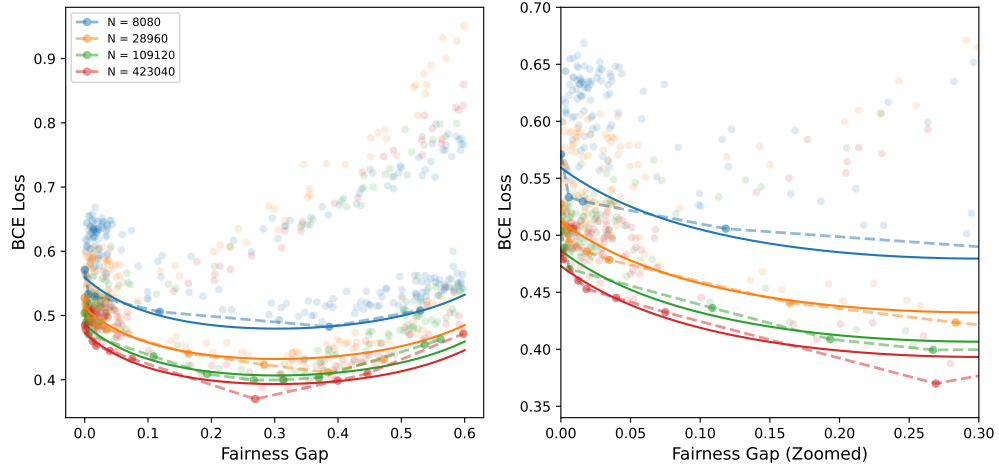


Figure 12: Pareto frontier for different model sizes under $(\pi = 0.4)$ and bias strength $\zeta = 2$. Each point corresponds to a trained model with a different fairness regularization weight λ . The dashed lines show the empirical Pareto frontier, created by finding the lower convex hull of all the points. The solid lines show fitted curves to the points on the Pareto frontier using Theorem 4.3 with $c = C_5 = 0.08$, $c' = C_6 = 0.43$, $c'' = C_7 = 0.85$, with bias $C_1 = 0.195$, $C_2 = 9$, $C_3 = 0.5$, and $C_4 = 0.5$. The left panel shows the frontier across the range of Δ , while the right panel zooms in on $\Delta \in [0, 0.3]$. The fitted curve mimics the empirical data well though it is imperfect. We found that there were many possible fits, depending on the precise choice. We show another possible fit in Figure 13 below.

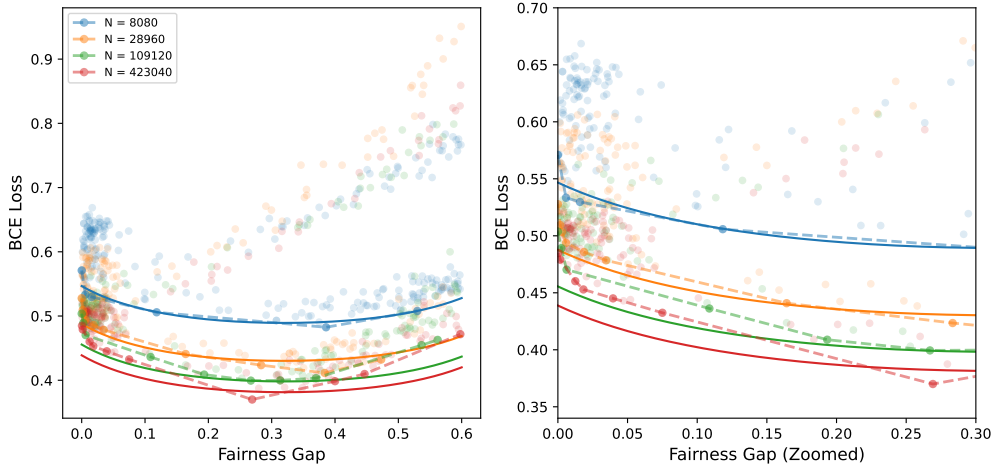


Figure 13: Pareto frontier for different model sizes under $(\pi = 0.4)$ and bias strength $\zeta = 2$. Each point corresponds to a trained model with a different fairness regularization weight λ . The dashed lines show the empirical Pareto frontier, created by finding the lower convex hull of all the points. The solid lines show fitted curves to the points on the Pareto frontier using Theorem 4.3 with $c = C_5 = 0.06$, $c' = C_6 = C_7 = 0.5$, $c'' = C_7 = 0.82$, with bias $C_1 = 0.18$, $C_2 = 11.25$, $C_3 = 0.8$, and $C_4 = 0.5$. The left panel shows the frontier across the range of Δ , while the right panel zooms in on $\Delta \in [0, 0.3]$. The fitted curve is intentionally chosen to lower bound the larger models. That is, it fits to the small model curve, then uses it to extrapolate the larger model curve; we do so to exhibit one possible way to fit the curves since our training procedure was not optimized for the larger models and, as such, our empirical Pareto frontier is likely not optimal. We show another possible fit in Figure 12.